



138  
559  
THS

2213842

LIBRARIES  
MICHIGAN STATE UNIVERSITY  
EAST LANSING, MICH 48824-1048

This is to certify that the  
thesis entitled

SPECTROSCOPIC CHARACTERIZATION OF 6-CYANO-2-  
NAPHTHOL FOR USE AS A CRYSTALLIZATION INITIATOR  
IN AQUEOUS SOLUTIONS

presented by

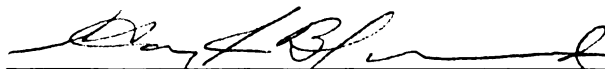
Alayna Michelle Goetsch

has been accepted towards fulfillment  
of the requirements for the

Master of  
Science

degree in

Chemistry



Major Professor's Signature

8/4/09

Date

**PLACE IN RETURN BOX** to remove this checkout from your record.  
**TO AVOID FINES** return on or before date due.  
**MAY BE RECALLED** with earlier due date if requested.

DATE DUE	DATE DUE	DATE DUE

**SPECTROSCOPIC CHARACTERIZATION OF 6-CYANO-2-NAPHTHOL FOR  
USE AS A CRYSTALLIZATION INITIATOR IN AQUEOUS SOLUTIONS**

**By**

**Alayna Michelle Goetsch**

**A THESIS**

**Submitted to  
Michigan State University  
in partial fulfillment of the requirements  
for the degree of**

**MASTER OF SCIENCE**

**Department of Chemistry**

**2004**



## **ABSTRACT**

# **SPECTROSCOPTIC CHARACTERIZATION OF 6-CYANO-2-NAPHTHOL FOR USE AS A CRYSTALLIZATION INITIATOR IN AQUEOUS SOLUTIONS**

By

Alayna Michelle Goetsch

Crystallization is a process that is complex and difficult to control. Among the experimental variables under our control are temperature, solution ionic strength,  $pH$ , and precipitant concentration. In a  $pH$  dependent system, a weak acid can be made to precipitate when the solution  $pH$  is set below the  $pK_a$ . A photoacid can be used as a (transient) source of protons in solution. When excited by light, the photoacid deprotonates, altering the local solution  $pH$ . The molecule 6-cyano-2-naphthol (6CN2) was used as a photoacid in this work in an attempt to modulate the solubility of adipic acid, a bifunctional weak acid. Spectroscopic characterization of 6CN2 was accomplished through the use of UV-VIS absorption and fluorescence and Time Correlated Single Photon Counting (TCSPC) measurements to evaluate the utility of 6CN2 as a potential crystallization initiator.

Copyright by  
Alayna Michelle Goetsch  
2004

**This work is dedicated to my parents for all of their support through my education and Mr. Hanson for teaching me the basics of chemistry through hands on laboratory experiences.**

## **ACKNOWLEDGMENTS**

I would like to first of all acknowledge Professor Gary Blanchard for all of his support and guidance during my graduate career. Without his enthusiasm and support, I would not have been able to complete my research for this thesis. Gary was an excellent teacher in helping me learn the laser system and how to help troubleshoot any other problems that arose during the research, of which there were many. I learned more about fixing instrumentation than I would ever imagine I ever had to know during a research project and yet was still able to complete work toward understanding the overall goal of my research project. I would also like to acknowledge the National Science Foundation and the Department of Energy through their grants for supporting the completion of this research. The graduate office in the Department of Chemistry has also been supporting me throughout my research career at Michigan State University. Dr. Tom Carter was also beneficial in helping with keeping the laser system operational and to supply appropriate software to do appropriate analysis and develop programs to help research go smoother. I would also like to thank my peers at and coworkers that helped me with ideas, support, and constructive comments about my research to help me expand and develop as a scientist.

# TABLE OF CONTENTS

	Page
<b>List of Tables.....</b>	<b>vii</b>
<b>List of Figures.....</b>	<b>Vii</b>
<b>List of Abbreviations.....</b>	<b>Xii</b>
<b>Chapter 1. Introduction.....</b>	<b>1</b>
1.1 Literature Cited.....	6
<b>Chapter 2. Dynamics of 6-cyano-2-naphthol in Aqueous Solutions. An Examination of Protonation/Deprotonation Dynamics and Aggregate Formation. ....</b>	<b>8</b>
2.1 Introduction.....	9
2.2 Experimental.....	10
2.3 Results and Discussion.....	15
2.4 Conclusions.....	46
2.5 Literature Cited.....	47
<b>Chapter 3. Using the Photoacid 6CN2 as an Initiator for the Crystallization of Adipic Acid. ....</b>	<b>49</b>
3.1 Introduction.....	50
3.2 Experimental.....	53
3.3 Results and Discussion.....	54
3.4 Conclusions.....	70
3.5 Literature Cited.....	72
<b>Chapter 4. Conclusions and Future Work</b>	<b>73</b>
4.1 Conclusions.....	75
4.2 Future Work.....	76
4.3 Literature Cited.....	77

## LIST OF TABLES

Table 2.1	Decay time constants and fractional contributions of the protonated and deprotonated forms of 6CN2. For both emission at 370 nm from the protonated form and emission at 440 nm from the deprotonated form, the data are of the form $f(t) = A_1 \exp(-t/\tau_1) + A_2 \exp(-t/\tau_2)$ . The physical significance of the signs of $A_1$ and $A_2$ are discussed in the text	29
Table 2.2	Reorientation time(s) for 6CN2 as a function of pH and at different excitation and emission wavelengths. In cases where multiple components of the anisotropy decay are seen	40
Table 3.1	Lifetime values of buffered $H_2AA/HAA^-$ solutions with $1.0 \times 10^{-5}$ M 6CN2. Excitation at 300 nm.	66
Table 3.2	Anisotropy values for buffered system with 6CN2 in solution. Excitation 300 nm, emission collection 440 nm	68

## LIST OF FIGURES

Figure 1.1	Energy equilibrium diagram of the photoacid of its ground and excited states. AH is merely an arbitrary photoacid.	4
Figure 1.2	Structures of some super photoacids Tolbert and coworkers synthesized. <sup>18</sup>	5
Figure 2.1	Schematic of the Time Correlated Single Photon Counter	12
Figure 2.2	The <i>pH</i> dependence of 6CN2 steady state absorbance spectrum. The spectra are shown in extinction units. All solutions were $1.0 \times 10^{-5}$ M in water, with <i>pH</i> controlled by concentration of HCl or NaOH. The protonated form is characterized by with $\epsilon_{\max} = 8890 \text{ L mol}^{-1} \text{ cm}^{-1}$ at 300 nm, and the deprotonated form has $\epsilon_{\max} = 3410 \text{ L mol}^{-1} \text{ cm}^{-1}$ at 325 nm.	17
Figure 2.3	<i>pH</i> Dependence of 6CN2 steady state emission spectra. All 6CN2 solutions were $1.0 \times 10^{-5}$ M and were excited at 300 nm. The emission band for protonated 6CN2 is centered at ca. 370 nm and the deprotonated form is centered near 440 nm. Solution acid and base concentrations are (a) 2.0 M HCl, (b) 1.5 M HCl, (c) 1.0 M HCl, (d) 0.75 M HCl, (e) 0.50 M HCl, (f) 0.1 M HCl, (g) 0.01 M HCl, (h) 0.001 M HCl, (i) 2 M NaOH. From these data we have determined $pK_a^* = 0.2$	18

Figure 2.4	Difference between excitation spectra of 6CN2 taken at the emission wavelengths of 440 nm and 500 nm, as a function of pH. Spectra were normalized to the intensity of the 234 nm band and the 260 nm band also seen in the pH dependence of the absorbance spectra seen in Figure 1. The spectral feature centered at ca. 300 nm is the absorption band of protonated 6CN2. The band at 350 nm is associated with a species that is neither the protonated or deprotonated form of 6CN2. This new feature increases in intensity with decreasing pH and is consistent with the existence of an aggregated 6CN2 species ( <i>vide infra</i> ). All solutions were $1.0 \times 10^{-5}$ M 6CN2 and [HCl] ranged from $10^{-3}$ M to 2 M.	20
Figure 2.5	The known equilibria between the excited states and ground state monomeric species	21
Figure 2.6	Solid lines: Steady state emission spectra of 6CN2 excited at 350 nm at selected HCl concentrations: (a) = 2 M HCl, (b) = 0.6 M HCl, (c) = $10^{-3}$ M HCl. Dashed line: Emission spectrum of a basic 6CN2 solution excited at 350 nm, (d) = $10^{-5}$ M NaOH	23
Figure 2.7	The new species and the possible pathways for deprotonation	25
Figure 2.8	(a) Time resolved emission spectra of 6CN2 in 0.1 M NaOH, (b) Time resolved emission spectra of 6CN2 in 2 M HCl. For both spectral data sets the time after excitation from top to bottom scans are 0, 20, 30, 50, 70, 90, 110, 120, 140, 160, 180, 200, 220, 240, 260, 310, 360, 410, 460 and 510 ps.	27
Figure 2.9	(a) Fluorescence lifetime of $1 \times 10^{-5}$ M 6CN2 in 2M HCl, excited at 300 nm, emission collected at 370 nm. (b) Fluorescence lifetime of $1 \times 10^{-5}$ M 6CN2 in $1.0 \times 10^{-5}$ M NaOH, excited at 300 nm, emission collected at 440 nm.	30
Figure 2.10	(a) Stern-Volmer plot for the protonated form of 6CN2 (o) and the deprotonated form of 6CN2 (•) quenched by $\text{Cl}^-$ . Lifetimes for the protonated form were acquired at 370 nm and 440 nm for the deprotonated form. (b) Stern-Volmer plot of quenching of the aggregate species by $\text{Cl}^-$ . Data were acquired using 350 nm excitation and 500 nm emission.	34



- Figure 2.11      Figure 2.11 : Time Resolved spectra of 6CN2 in  $pH = 0.25$  (0.6 M HCl), during the first 500 ps of the molecule's lifetime. Peak maximum at first is at 420nm and dies down. There is a faint trace of peak at 500nm. The time after excitation from top to bottom scans are 0, 20 , 30, 50, 70, 90, 110, 120, 140, 160, 180, 200, 220, 240, 260, 310, 360, 410, 460 and 510 ps. 36
- Figure 2.12      (a) Fluorescence lifetime of  $1 \times 10^{-5} M$  6CN2 in 0.6M HCl, excited at 350 nm, emission collected at 420 nm. (b) Fluorescence lifetime of  $1 \times 10^{-5} M$  6CN2 in 0.6M HCL, excited at 350 nm, emission collected at 500 nm. 38
- Figure 2.13      6CN2 equilibria relevant to this work. Top pane: Protonation/deprotonation equilibria with ground state and excited state  $K_a$ 's indicated. Absorption and emission maxima are indicated. Bottom pane: Proposed aggregation equilibria. We have implied the identity of the aggregate species to be a dimer for reasons of physical and chemical plausibility (see text). 45
- Figure 3.1      Adipic acid ( $H_2AA$ ) and adipate anion ( $AA^{2-}$ ) and hydrogen adipate anion ( $HAA^-$ ) equilibrium.<sup>19</sup> The first  $pK_a = 4.4$  and the second  $pK_a = 5.4$ . 51
- Figure 3.2      Steady state spectra of samples for excitation at 300 nm, solid line is spectrum taken prior to UV exposure and the dotted line is the spectrum taken after the sample is exposed to UV light. (a) Is  $H_2AA$  and  $Na_2AA$  supersaturated and no 6CN2. (b) Same concentration of  $H_2AA$  and  $Na_2AA$  with also  $1.0 \times 10^{-5} M$  6CN2 added. 56
- Figure 3.3      Steady state spectra of 6CN2 in buffered  $H_2AA/HAA^-$  solutions for excitation at 300 nm with spectra taken in time intervals between 2 hrs to 12 hours. All spectra are identical. Solution not exposed to UV light. 57
- Figure 3.4      Steady state spectra of 6CN2 in buffered  $H_2AA/HAA^-$  solution with concentration ratio of  $H_2AA/Na_2AA$  10:1 for excitation at 360 nm with spectra taken in time intervals between 2 hrs to 12 hours after exposure. (a) Solution kept in the dark (b) Solution under UV exposure. Concentration of adipic acid to sodium adipate is 10:1. 59

- Figure 3.5      Steady state spectra of 6CN2 with H<sub>2</sub>AA/Na<sub>2</sub>AA concentration ratio 30:1 and under UV exposure. The buffered H<sub>2</sub>AA/HAA<sup>-</sup> and 6CN2 solution (a) 300 nm excitation (b) 360 nm excitation. 61
- Figure 3.6      Steady state spectra 6CN2 and H<sub>2</sub>AA with no Na<sub>2</sub>AA added in aqueous solution exposed to UV light. The buffered H<sub>2</sub>AA/HAA<sup>-</sup> solution (a) for excitation at 300 nm (b) for excitation at 360 nm. 63
- Figure 3.7      Steady state spectra 6CN2 in buffered H<sub>2</sub>AA/HAA<sup>-</sup> solution for excitation at 350 nm. The solution was exposed to 355 nm UV light powered by a laser for 5 minutes and then allowed to sit in the dark after exposure. 65
- Figure 3.8      TCSPC data for excitation at 300nm, emission at 440nm. Buffered H<sub>2</sub>AA/HAA<sup>-</sup> solution with concentration ratio of H<sub>2</sub>AA and Na<sub>2</sub>AA 30:1. The 6CN2 was in 1.0x10<sup>-5</sup>M concentration. 67
- Figure 3.9      Lifetime of H<sub>2</sub>AA solution with no Na<sub>2</sub>AA and 10<sup>-5</sup> M 6CN2 for excitation at 300nm emission collection at 440 nm. 69

## LIST OF ABBREVIATIONS

**TCSPC.....Time Correlated Single Photon Counting**

**6CN2.....6-cyano-2-naphthol**

**H<sub>2</sub>AA.....Adipic acid**

**Na<sub>2</sub>AA.....Sodium adipate**

**TAC.....Time to amplitude converter**

**CFD.....Constant fraction discriminator**

**PMT.....Photomultiplier tube**

**MCA.....Multichannel analyzer**

**MCP.....Microchannel plate**

# **Chapter 1**

## **INTRODUCTION**

Many industries and pharmaceutical companies use crystallization to purify chemicals. The range of materials purified by crystallization underscores the importance of this fundamental chemical process. The details of crystallization, such as growth kinetics and crystal size, depend on the system properties, such as solute identity, solute concentration, solution ionic strength, dielectric response, *pH*, and temperature. Crystallization, in many cases, is influenced by the kinetics of crystal nucleation and growth, and in essentially all cases, initiation of crystallization relies on an external event, such as shockwave or the introduction of a nucleation impurity. The ultimate goal of our work is to devise a means of initiating crystallization in a chemically controlled manner. This thesis represents only the initial stages of this effort, focusing on the properties of a photoacid.

Nucleation and crystal growth affect how large a crystal will be during the crystallization process. If nucleation dominates, many small particles will result. If crystal growth dominates, fewer larger crystals are obtained<sup>1</sup>. Large crystals are desirable from a chemical processing perspective. In order to produce large crystals, the appropriate balance between nucleation and growth needs to be achieved. Nucleation and growth are factors that are controlled by a variety of system parameters with each system requiring optimization. Much effort has been expended on investigating solution properties prior to crystallization, with an

eye toward understanding pre-crystallization organization.<sup>2-8</sup> Berglund *et al*<sup>9</sup> started investigation of crystallization events with the use of a fluorescent probe. Blanchard<sup>10-14</sup> and coworkers have also used fluorescent probes and spectroscopic techniques, such as Time Correlated Single Photon Counting (TCSPC), to gain insight into crystallization precursors in glucose and adipic acid solutions.

One solution property that can be used to control crystallization in aqueous systems is *pH*. Carboxylic acid solubility depends on their charge. Anionic, deprotonated species are typically more soluble in aqueous solution than their protonated (neutral) forms. Reducing the *pH* of such solutions to the point where  $pH < pK_a$  of the weak acid can serve to initiate crystallization by increasing the concentration of the less soluble, protonated form of the carboxylic acid. The most well established means of controlling *pH* is either through the addition of strong acids or bases to solution, or by the use of a buffer. Both of these methods involve mixing and poorly controlled concentration gradients in the crystallizing solution, thereby limiting the control that can be exercised over crystallization. An alternative means to alter solution *pH*, albeit on a transient basis, is to use organic photoacids in solution and with these species, control the solution *pH* by means of light. The ultimate success of this approach is far from being assured and rests on the kinetics of carboxylic acid deprotonation being slow relative to the photon-induced proton production from the photoacid. The first step in evaluating the feasibility of this approach is to understand the protonation/deprotonation dynamics of the photoacid.



The difference value between the excited state equilibrium constant and the ground state equilibrium constant varies within the structural identity of the hydroxyarene. In 1994, Tolbert<sup>18-19</sup> and coworkers synthesized a series of photoacids with extremely large differences between  $pK_a$  and  $pK_a^*$ , yielding some  $pK_a^*$  values below zero. This family of molecules is referred to as super photoacids,<sup>20</sup> and all of the members reported to date are substituted hydroxynaphthalenes (Figure 1.2).

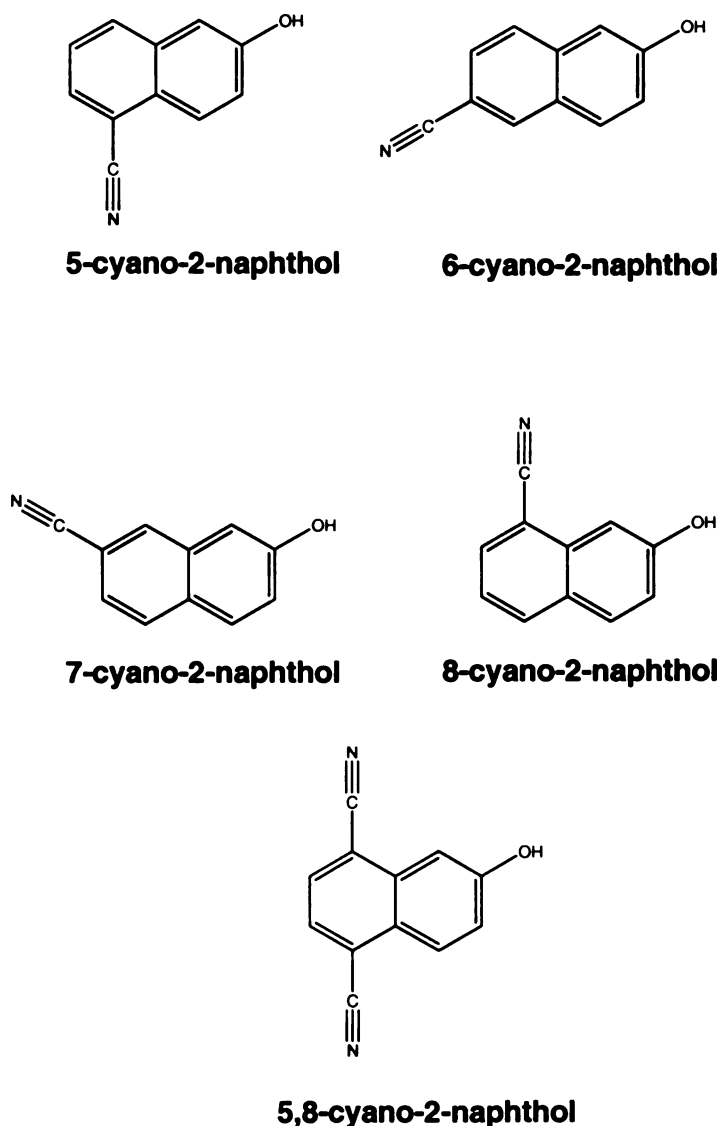


**Figure 1.2: Structures of some super photoacids Tolbert and coworkers synthesized.<sup>18</sup>**

These 2-naphthols possess cyano group(s) on their distal ring. Different locations of the cyano group(s) on the 2-naphthol ring structure results in variations in  $pK_a^*$  values. Tolbert has reported that these photoacids are strong proton donors in a variety of solvents<sup>21-23</sup> and their protonation/deprotonation equilibria can be monitored spectroscopically.<sup>24-26</sup> 6-cyano-2-naphthol (6CN2) has not been studied as extensively as some of the other substituted 2-naphthols,<sup>27-30</sup> but 6CN2 is available commercially and its spectroscopic and photoacid properties are consistent with the other cyano-naphthols.

We will use 6CN2 as a proton donor in aqueous solutions of an organic acid. We use a laser, already incorporated in our single photon counting system to excite 6CN2, producing protons in the light path. The spectral changes of 6CN2 on photoexcitation provide information on the kinetics of deprotonation and reveal the conditions under which this chromophore may prove useful.



## **1.1 Literature Cited**

1. Skoog, D.A.; Holler, F.J.; West, D. M.; *Analytical Chemistry: An Introduction 7<sup>th</sup> Ed.* Harcourt, Inc. Orlando, Florida **2000** 182
2. Myerson, A.S.; Sorrel, L.S.; *AIChE J.* **1982**, *28*, 778
3. Sorrel, L.S.; Myerson, A.S.; *AIChE J.* **1982**, *28*, 772
4. Chang, Y.C.; Myerson, A.S.; *AIChE J.* **1985**, *31*, 980
5. Chang, Y.C.; Myerson, A.S.; *AIChE J.* **1986**, *32*, 1567
6. Chang, Y.C.; Myerson, A.S.; *AIChE J.* **1986**, *32*, 1747
7. Larson, M. A.; Garside, J.; *Chem. Eng. Sci.* **1986**, *41*, 1285
8. Larson, M. A.; Garside, J.; *J. Crystal Growth.* **1986**, *76*, 88
9. Chakraborty, R.; Berglund, K. A.; *AIChE. Symp. Ser.* **1991**, *284*, 113
10. Rasimas, J.P.; Berglund, K. A.; Blanchard, G. J.; *J. Phys. Chem.* **1996**, *100*, 7220
11. Rasimas, J.P.; Berglund, K. A.; Blanchard, G. J.; *J. Phys. Chem.* **1996**, *100*, 17034
12. Tulock, J. J.; Blanchard, G. J.; *J. Phys. Chem. B* **1998**, *102*, 7148
13. Tulock, J. J.; Blanchard, G. J.; *J. Phys. Chem. A* **2000**, *104*, 8340
14. Kelepouris, L.; Blanchard, G. J.; *J. Phys. Chem. A* **2000**, *104*, 7261
15. Förster, T.; *Z. Elektrochem.* **1950**, *54*, 311
16. Bell, R.P.; *The Proton in Chemistry, 2<sup>nd</sup> Edition.* Cornell University Press, New York. **1973**
17. Caldin, E.; Gold, V. *Proton Transfer Reactions.* Chapman and Hall, New York **1975**
18. Tolbert, L. M.; Haubrich, J.M.; *J. Am. Chem. Soc.* **1994**, *116*, 10593
19. Tolbert, L. M.; Haubrich, J.M.; *J. Am. Chem. Soc.* **1990**, *112*, 8163
20. Tolbert, L. M.; Solntsev, K. M.; *Acc. Chem. Res.* **2002**, *35*, 19

21. Solntsev, K. M.; Huppert, D.; *J. Phys. Chem. A* **1999**, *103*, 6984
22. Solntsev, K. M.; Huppert, D.; *J. Am. Chem. Soc.* **1998**, *120*, 7981
23. Solntsev, K. M.; Huppert, D.; Agmon, N.; Tolbert, L. M.; *J. Am. Chem. Soc.* **2000**, *104*, 46580
24. Knochenmuss, R.; Solntsev, K. M.; Tolbert, L. M.; *J. Phys. Chem. A* **2001**, *105*, 6393
25. Cohen, B.; Segal, J.; Huppert, D.; *J. Phys. Chem. A* **2002**, *106*, 7462
26. Solntsev, K. M.; Tolbert, L. M.; Cohen, B.; Huppert, D.; Yoshihito, H.; Feldman Y.; *J. Am. Chem. Soc.* **2002**, *124*, 9046
27. Solntsev, K. M.; Agmon, N.; *Chemical Physics Letters*. **2000**, *320*, 262
28. Huppert, D.; *J. Phys. Chem. A* **1997**, *101*, 4602
29. Agmon, N.; Rettig, W.; Groth, C.; *J. Am. Chem. Soc.* **2002**, *124*, 1089
30. Barroso, M.; Arnaut, L. G.; Fornosinho, S.J.; *Journal of Photochemistry and Photobiology. A: Chemistry* **2002**, *154*, 13

## **Chapter 2**

### **Dynamics of 6-Cyano-2-Naphthol in Aqueous Solutions. An Examination of Protonation/Deprotonation Dynamics and Aggregate Formation.**

#### **Summary**

We report on the behavior of 6-cyano-2-naphthol (6CN2) in aqueous solutions. 6CN2 is a well known photoacid and we are interested in its ability to produce local changes in solution  $pH$  upon excitation. We have measured the ground state and excited state  $pK_a$  values for 6CN2 and have studied the steady state and transient optical properties of this chromophore as a function of  $pH$ . We use transient spectral dynamics measurements to find the average deprotonation time for 6CN2 as a function of solution  $pH$  and provide evidence for the existence of a transient aggregate with a spectroscopic response suggesting it is a dimer. With this information we are able to characterize the multiple equilibria responsible for the spectroscopic behavior of 6CN2.

## 2. 1 Introduction

Photoacids are a family of compounds that has attracted significant attention for both practical and fundamental reasons. The substituted 2-naphthols are one group of photoacids that has been studied extensively because of the anomalously large difference in the acidity of their hydroxyl proton in the ground and excited electronic states.<sup>1-15</sup> 2-Naphthols are known to exhibit this effect based on the ability of the excited state anion to be resonance-stabilized, giving rise to  $pK_a^*$  values more than 5 units lower than  $pK_a$  values.<sup>3,10</sup> Simple resonance structure predictions indicate that the placement of electron-withdrawing substituents at certain positions on the distal ring of 2-naphthol will result in an enhancement in the difference between  $pK_a$  and  $pK_a^*$  values, and this prediction has been verified with several positional substitutions and with several different electron withdrawing groups.<sup>2,12</sup> Of these so-called “super photoacid” compounds, 6-cyano-2-naphthol (6CN2) has emerged as a relatively well behaved member, and this compound is the focus of the work we report here.

A substantial reason for the interest in super photoacids lies in their ability to protonate solvents, facilitating the study of photoinduced proton exchange dynamics.<sup>2,3,5-7,9,12-15</sup> We are interested in 6CN2 because of its ability to alter the local pH of a solution phase environment upon excitation. Such a local transient decrease in pH could serve to mediate the solubility of certain species in solution and 6CN2 could thus function as a “photo-trigger” for precipitation events, depending on the proton association and dissociation kinetics of the putative

precipitating moiety. Prior to using 6CN2 to photoinduce precipitation, however, we need to understand its optical properties and protonation / deprotonation dynamics. We report here on our measurements of the excited state  $pK_a$  value for this chromophore in aqueous solution and on the time-domain excited state protonation / deprotonation behavior as a function of  $pH$ . Several reports in the literature have hinted at the existence of substituted 2-naphthol aggregates in solution,<sup>7,12</sup> but we are unaware of any detailed information on such species. We report here on our direct measurement of the linear optical properties of an aggregated species. Our time-resolved reorientation and lifetime data provide insight into the lifetime of this aggregate and suggest that excitation of the aggregate gives rise to spontaneous dissociation.

## 2.2 Experimental

*Chemicals.* 6-Cyano-2-naphthol (6CN2) was obtained from TCI America and used as received. The solutions with varying  $pH$  of 6CN2 were prepared using deionized water obtained in-house. For all time-resolved measurements, the concentration of 6CN2 was  $10^{-5}$  M, with the  $pH$  of the solutions being determined by the HCl or NaOH concentration. Electronic grade concentrated HCl was purchased from CCI.

*Steady state spectroscopy.* Absorption measurements were made using a Varian Cary model 300 double beam UV-visible absorption spectrometer. All measurements were made with 1 nm resolution. Emission and excitation spectra were recorded using a JY-Spex Fluorolog 3 emission spectrometer. For all

measurements, the excitation bandwidth was 2 nm and the emission bandwidth was 2 nm.

*Time-Correlated Single Photon Counting (TCSPC) Spectrometer.* The spectrometer used for the lifetime and dynamical measurements was similar to one described in detail before and it is shown in Figure 2.1<sup>16</sup>. The excitation light pulses are produced by a synchronously pumped, cavity-dumped dye laser (Coherent 702-2, 5 ps pulses, 4 MHz repetition rate). The dye laser is excited by the second harmonic of the output of a cw mode-locked Nd:YAG laser (Coherent Antares 76S, 100 ps pulses, 76 MHz repetition rate). Samples were excited at 300 nm (Rhodamine 6G dye, Kodak, KDP Type I SHG) and 350 nm (LDS698 dye, Exciton, KDP Type I SHG).

The output of the dye laser in this configuration was ~ 90 mW average power with pulses of 5 ps FWHM. The output of the dye laser was divided by a beam splitter with 90% of the output being sent for excitation of the sample and 10% used as a reference pulse. This pulse sent into a fiber optic delay line allowing for a temporal delay between the signal and the reference. The KDP crystals used introduces astigmatism that is compensated by a plano-convex cylindrical lens followed by filtering through a colored glass filter to remove longer wavelength of light from the second harmonic light produced. The polarization of the light is then rotated by a fused silica half-wave rhomb (CVI Laser Corporation) to 0° to make the light vertically polarized. The polarized UV light is focused into the sample with an 88mm focal length bi-convex fused silica lens that results in an average power at the sample of  $\leq 1\text{mW}$ . For all experiments

emission is collected at  $90^\circ$  with respect to the incident light with a reflecting microscope objective (Ealing x36/0.5) followed by a Glan-Taylor (G-T) prism for selection of polarization. The polarization angles collected were at  $0^\circ$  and  $90^\circ$  for anisotropy measurements and  $54.7^\circ$  for rather lifetime measurements. This G-T prism was rotated by a motorized rotation stage (Newport Motion Controller Model MM3000). The controller was operated using LabVIEW 7.0 software. The selected polarization is then sent through a pseudo polarization scrambler and focused into a subtractive double monochromator (CVI). The monochromator is in communication to the computer and controlled by LabVIEW 7.0 software.

The detection electronics have been described in detail elsewhere<sup>17</sup>, and the significant features are reviewed here briefly. For detection, a Hamamatsu (R3809U-50) cooled two plate microchannel plate photomultiplier tube (MCP-PMT) is used and operated at a bias of - 3.10 kV. The signal produced from the detector is sent to one channel of a four channel constant fraction discriminator (CFD, Tennelec TC455) for processing prior to its input to the time-to-amplitude converter (TAC, TC864). We operate the TAC in “reverse mode”; the signal from the MCP-PMT serves as the start signal and the stop signal originates from the portion of the laser pulse that is split into the fiber optic delay line. This custom made optical delay consists of varying lengths of fiber terminating in detection by an avalanche photodiode detector (PD, RCA C30902E) whose signal is routed into a second channel of the CFD. The output of the CFD reference signal is electronically delayed (Tennelec TC412A) and sent to the TAC stop channel. This configuration of the start and stop channels is termed “reverse mode” and

helps to eliminate pulse pile-up, and ensures operation of the TAC in a linear conversion range. The valid conversions of the TAC output are displayed on an oscilloscope (Tektronix 2230) and rate meter (Tennelec TC525) and sent to a multichannel analyzer (MCA, Tennelec PCA-II) for collection.

Emission was monitored using a 10 nm collection bandpass for each wavelength of interest. The collection wavelength was stepped by computer control and individual time-domain decays were collected to generate time-resolved spectral profiles. Fluorescence was collected at 0°, 54.7°, and 90° with respect to the vertically polarized excitation pulse. The instrument response function for this system is typically 35 ps FWHM and transients measured range from ~100 ps to ~6 ns. We did not deconvolute the instrument response function from the experimental data. The shortest reorientation times we measure are on the order of 50 ps, and because we can recover the entire anisotropy decay, loss of the initial portion of the decay does not affect the accuracy of our determinations.



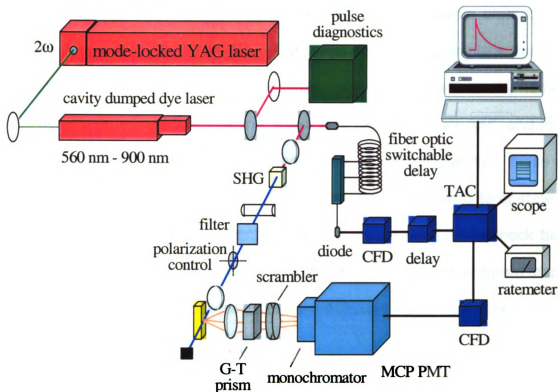


**Figure 2.1: Schematic of the Time Correlated Single Photon Counter**

A computer program written using National Instruments LabVIEW version 7.0<sup>®</sup> software was designed to automate the TCSPC system. For each polarization collected an instrument response function was also acquired and both data sets stored to the computer. This program created many ASCII data files, which created a need manage the data more effectively. LabVIEW 7.0<sup>®</sup> has a Report Generation analysis package that has commands to open Microsoft Excel<sup>®</sup>. A computer program was designed through LabVIEW 7.0<sup>®</sup> to place all magic angle/lifetime data in the appropriate Excel worksheets. In the Excel file created, one worksheet was labeled "Responses" with the date attached to the sheet and another worksheet was labeled "Lifetime" with the date attached to the

sheet. The Excel file was then saved with the same file name created in the original program to run the TCSPC. Code was also developed to place the 0° and 90° responses and data files into a separate Excel program with similar names to the worksheet, except the “Lifetime” sheet was named “Anisotropy”, and to add on continuously if the program was started and stopped frequently. These sub-programs were placed into the TCSPC data collection programs to operate and collect the data for the instrument. Code was also developed to check before data collection if the name provided already exists, if it did, the program stopped and asked the user to proceed with a different file name and start over.

## **2.3 Results and Discussion**

The purpose of this work is to establish an understanding of the protonation and deprotonation dynamics of 6CN2. Ultimately, we would like to mediate the solubility of compounds, such as adipic acid in aqueous solution, by means of optically induced changes in solution pH. Any such change would be transient, of course, and the ability to mediate solubility on timescales longer than the excited state lifetime of a photoacid would hinge on the protonation and deprotonation kinetics of the proton acceptor. As a first step in evaluating the feasibility of any such approach to mediating solubility, we must understand the behavior of the photo-induced proton donor. The excited state proton exchange dynamics of cyano-2-naphthol derivatives have been examined extensively and there have been several useful experimental and theoretical examinations of the characteristic photoacidity of this family of compounds.<sup>1,2,5-14</sup> Our experimental data suggest that the time scale for proton transfer is on the order of tens to

hundreds of ps, depending in some instances on solution pH. In several studies, aggregation phenomena have been invoked to explain long-lived features in the transient optical response,<sup>7,12</sup> but the putative aggregates remain poorly characterized, especially in polar solvents such as water. We have also found evidence for the aggregation of 6CN2 at low pH, and our steady state and time-resolved spectroscopic data provide some insight into its structural identity and persistence time in solution. We propose a series of equilibria for 6CN2 in aqueous solution to account for our findings. We have used steady state and time-resolved spectroscopic measurements to obtain this information, and we consider these measurements individually.

*Steady state spectroscopic results.* The absorption data shown in Figure 2.2 indicate that the optical absorption spectrum of 6CN2 in aqueous solution does not vary substantially with pH over the range of  $-0.3 \leq \text{pH} \leq 3.0$ . The  $\text{pK}_a$  of 6CN2 has been reported to be 8.40<sup>12</sup> and we have not determined this quantity experimentally because it does not lie within the pH range of the experiments we perform here. We note that the absorption spectrum of 6CN2 does change when the chromophore is deprotonated (Figure 2.2), but we do not access this pH region in our experiments.

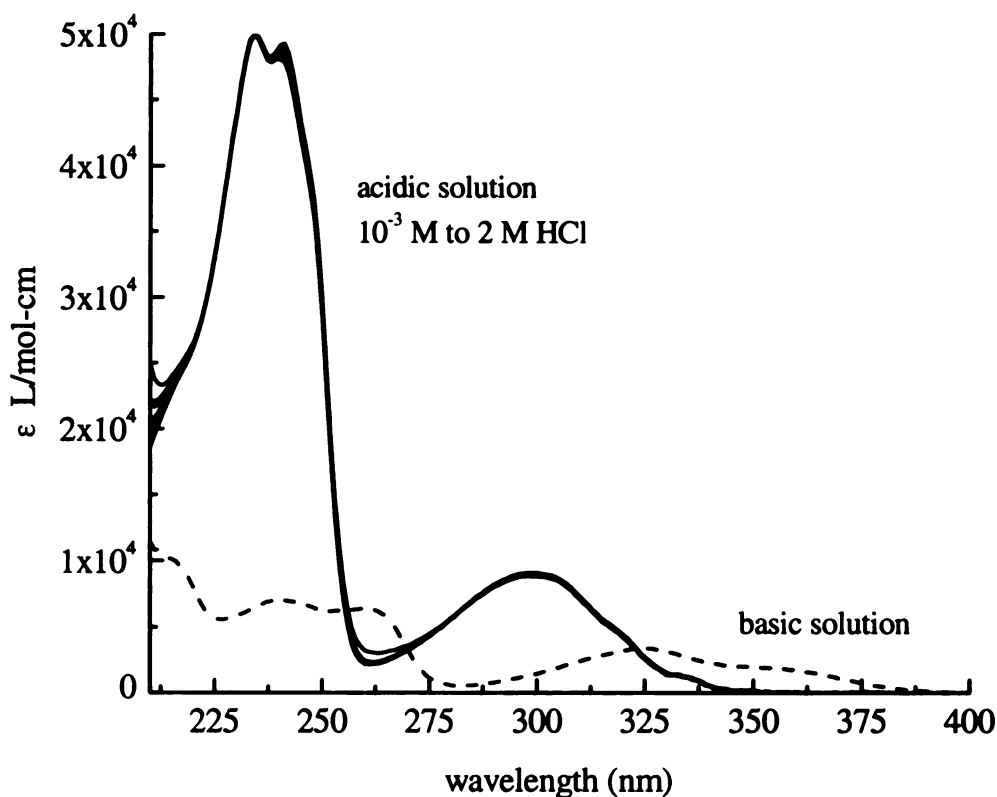


**Figure 2.2:** The pH dependence of 6CN2 steady state absorbance spectrum. The spectra are shown in extinction units. All solutions were  $1.0 \times 10^{-5}$  M in water, with pH controlled by concentration of HCl or NaOH. The protonated form is characterized by with  $\epsilon_{\text{max}} = 8890 \text{ L mol}^{-1} \text{ cm}^{-1}$  at 300 nm, and the deprotonated form has  $\epsilon_{\text{max}} = 3410 \text{ L mol}^{-1} \text{ cm}^{-1}$  at 325 nm.

We have determined the  $pK_a^*$  value for 6CN2 experimentally by means of fluorescence titration<sup>18</sup> because there is some uncertainty in the literature regarding its value, but more importantly because it lies within the pH range we access and it is thus important to have an accurate measure of this quantity under our experimental conditions. Figure 2.3 shows the pH dependence of the emission spectra of 6CN2. The band with a maximum near 370 nm is associated with the protonated form of 6CN2 and the 440 nm band arises from the deprotonated form. This assignment is consistent with

the Förster model,<sup>2</sup> which predicts a spectral red-shift of the emission band on deprotonation. We have normalized the areas under these spectra and an isoemissive point is seen at ~405 nm. From these data we find  $pK_a^* = 0.25$  for 6CN2 in water. Our value is in agreement with other reports which place  $0.2 \leq pK_a^* \leq 0.5$ . As has been noted elsewhere, the Förster shift can be used to estimate the change in  $pK_a$  of a molecule on excitation, and for 6CN2, this model provides an underestimate of the  $pK_a$  change.<sup>12,15</sup>

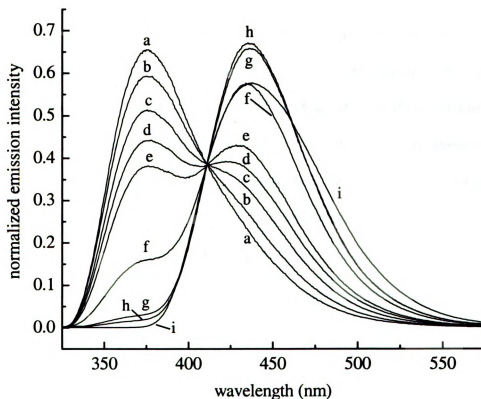


**Figure 2.3:** pH Dependence of 6CN2 steady state emission spectra. All 6CN2 solutions were  $1.0 \times 10^{-5}$  M and were excited at 300 nm. The emission band for protonated 6CN2 is centered at ca. 370 nm and the deprotonated form is centered near 440 nm. Solution acid and base concentrations are (a) 2.0 M HCl, (b) 1.5 M HCl, (c) 1.0 M HCl, (d) 0.75 M HCl, (e) 0.50 M HCl, (f) 0.1 M HCl, (g) 0.01 M HCl, (h) 0.001 M HCl, (i) 2 M NaOH. From these data we have determined  $pK_a^* = 0.2$

The absorption spectral data (Figure 2.2) indicate that the  $S_1 \leftarrow S_0$  absorption maximum of protonated 6CN2 is centered at 300 nm. Because the  $pK_a$  and  $pK_a^*$  are so different, we excite exclusively protonated 6CN2 in this work, and monitor both the protonated and deprotonated excited species, and the exchange of population between them. We will discuss these spectral relaxation studies below. In addition to the dominant 300 nm absorption band, we have identified a weak absorption feature centered near 350 nm, which is present only at low pH. This 350 nm absorption band is associated with an emission band in the region of 500 nm. In an effort to identify the origin of the 350 nm absorption band, we have acquired excitation spectra, monitoring emission intensity at 430 nm and 500 nm. The 430 nm emission spectra are associated with deprotonated 6CN2\* and the 500 nm emission spectra are associated with a different, previously unidentified species. By taking the difference between the excitation spectra acquired for the two different emission wavelengths, we can resolve the 350 nm absorption band. We show these difference spectra in Figure 2.4, normalized for constant oscillator strength in this spectral window. These data contain several interesting features. Near pH 3,

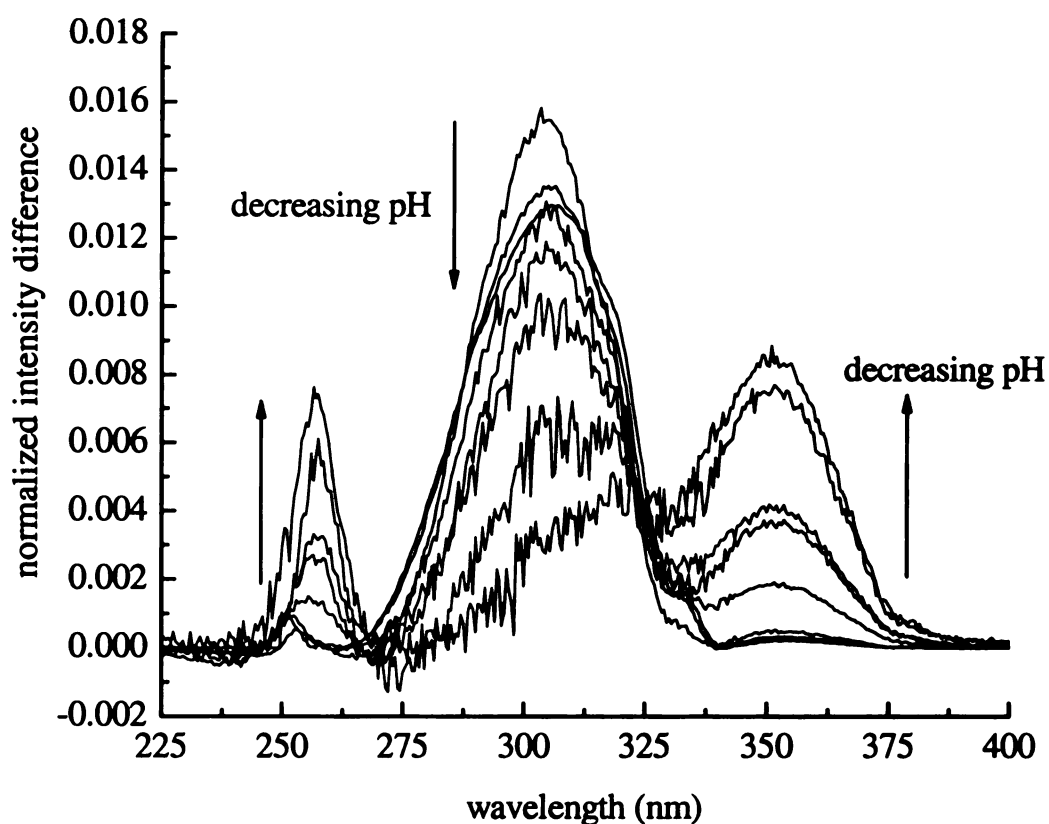


**Figure 2.4:** Difference between excitation spectra of 6CN2 taken at the emission wavelengths of 440 nm and 500 nm, as a function of *pH*. Spectra were normalized to the intensity of the 234 nm band and the 260 nm band also seen in the *pH* dependence of the absorbance spectra seen in Figure 1. The spectral feature centered at ca. 300 nm is the absorption band of protonated 6CN2. The band at 350 nm is associated with a species that is neither the protonated or deprotonated form of 6CN2. This new feature increases in intensity with decreasing *pH* and is consistent with the existence of an aggregated 6CN2 species (*vide infra*). All solutions were  $1.0 \times 10^{-6}$  M 6CN2 and [HCl] ranged from  $10^{-3}$  M to 2 M.

the difference in intensity between the two excitation wavelengths is the result of the different absorbance of 6CN2 at the two excitation wavelengths. At *pH* 3, essentially the only species present is the protonated ground state – the 300 nm excitation band is in excellent agreement with the absorbance spectra shown in Figure 2.2. As the *pH* is decreased, we observe a diminution of the 300 nm excitation band and a corresponding increase in bands centered at 350 nm and

255 nm. It is clear from these difference spectra that there is a substantial increase in the 350 nm band as the pH is lowered, indicating that the species responsible for this subtle spectral feature we observe is associated with some protonated form of 6CN2. A schematic of the equilibria between the ground state and excited state forms of 6CN2 is shown in Figure 2.5.

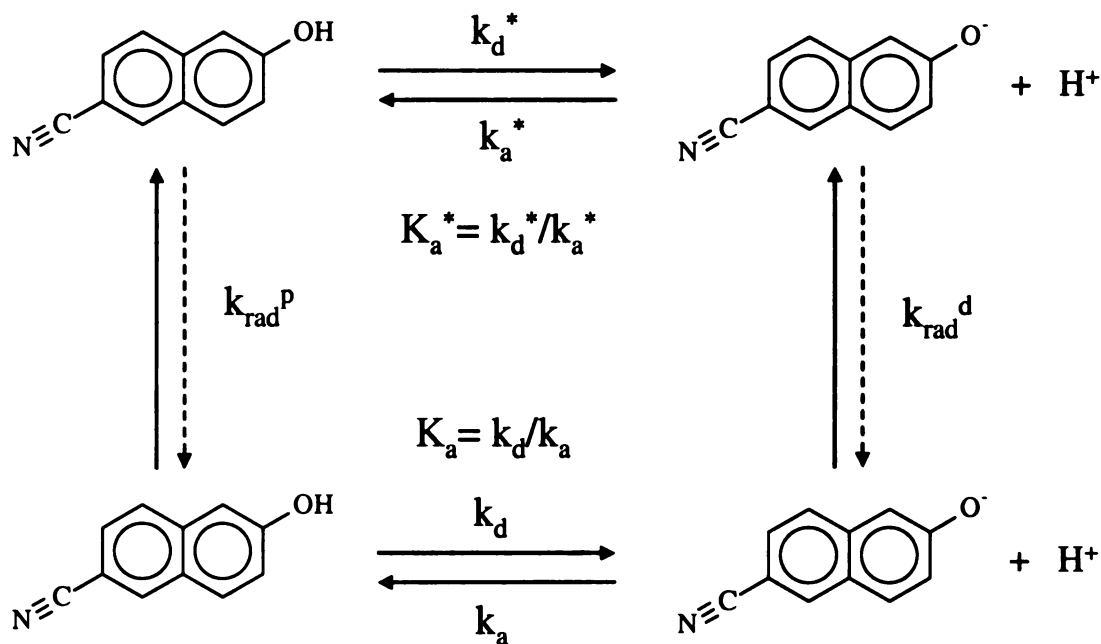


**Figure 2.5: The known equilibria between the excited states and ground state monomeric species.**

While it is tempting to interpret the difference spectra shown in Figure 2.4 in terms of an equilibrium between two species (*e.g.* two different protonated forms) due to the form of these spectra, making such an interpretation is not possible and not consistent with the spectra from which Figure 2.4 is derived. The form of the difference spectra depends on the collection wavelengths used and inferring equilibrium information from Figure 2.4 is not possible. The



excitation spectra used in the creation of Figure 2.4 show the dominant species for all measurements to be protonated 6CN2.

We excite the sample at 350 nm and measure the emission spectral profile associated with this new band. We observe that the emission band associated with the 350 nm absorption feature has a maximum near 500 nm and exhibits a *pH* dependence (Figure 2.6). For high *pH* solutions we obtain the emission spectrum of the deprotonated form of the 6CN2 chromophore (Figure 2.6) and do not resolve any contribution from the 500 nm emission feature. There is spectral overlap between the 300 nm absorption band of protonated 6CN2 and the 350 nm feature, resulting in a signal from both the monomeric species and the new species appearing when the sample is excited at 350 nm. Based on the spectral shift data and the *pH*-dependence for the 350 nm absorption and 500 nm emission bands, we believe these features are those of an aggregate of at least two 6CN2 molecules.

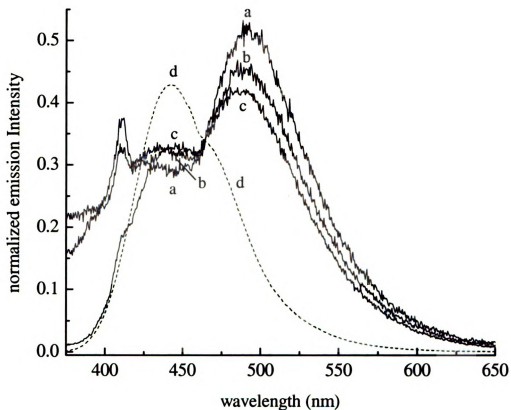


**Figure 2.6:** Solid lines: Steady state emission spectra of 6CN2 excited at 350 nm at selected HCl concentrations: (a) = 2 M HCl, (b) = 0.6 M HCl, (c) =  $10^{-3}$  M HCl. Dashed line: Emission spectrum of a basic 6CN2 solution excited at 350 nm, (d) =  $10^{-5}$  M NaOH.

If the 350 nm absorption band and 500 nm emission band are indeed associated with an aggregate, the pH dependence of these bands should provide some insight into possible structure(s) of the aggregate. We note that the amount of aggregate present in solution is related to the solution proton concentration. The form of the absorption and emission data are not consistent with the 350 nm species being a doubly protonated form of 6CN2. Rather, the pH-dependence indicates the aggregate is formed from neutral

(monoprotonated) 6CN2 molecules. The simplest aggregate would be a dimeric species and we do not observe any precipitation of 6CN2 or other species in low pH solutions. The existence of an aggregate is not unexpected based on the dipolar nature of 6CN2, with a face-to-face arrangement of opposing dipole moments being one possible structure. This type of aggregate structure could give rise to a modest lifetime for an aggregate, depending on the strength of interaction, and our experimental data suggest this to be the case. Reasons for the subtlety of the aggregate optical response may be that it is either short-lived or that photoexcitation of the aggregate constituent(s) leads to dissociation. In the latter picture, the deprotonation of one member of the aggregate would give rise to an  $\text{O}^-$  functionality in close proximity to a nucleophilic  $\text{-C}\equiv\text{N}$  moiety on another 6CN2 molecule. Repulsive interactions for such a structure would force the dimer constituents apart, leaving a deprotonated 6CN2\* and a protonated ground state 6CN2. This explanation for the 350 and 500 nm spectral features is speculative, and we can gain some additional insight into its behavior using time-domain spectroscopy. Specifically, excitation of the 350 nm feature at low pH will select for the putative aggregate, and its transient optical properties may provide insight into its lifetime. The simplest aggregate would be a dimeric species and we do not observe any precipitation of 6CN2 or other species in low pH solutions. The existence of an aggregate is not unexpected based on the dipolar nature of 6CN2, with a face-to-face arrangement of opposing dipole moments being one likely structure. There are two possible pathways that this particular dimer could split apart and are shown in Figure 2.7.

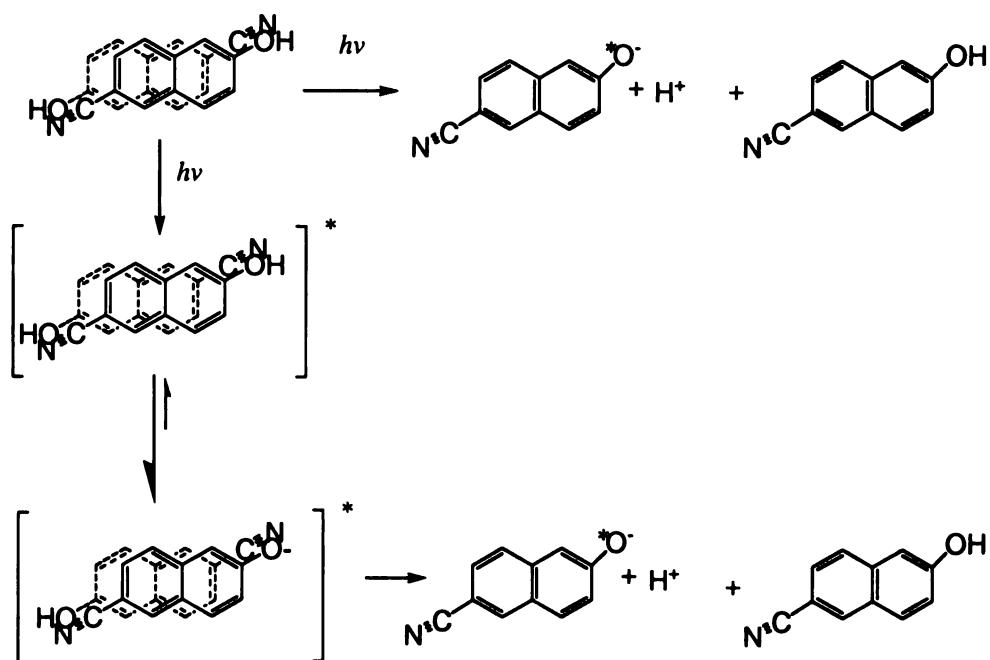


**Figure 2.7: The new species and the possible pathways for deprotonation**

The first pathway suggests that upon excitation, there is no lifetime of the dimer and it completely goes to an excited form of the deprotonated monomer and a ground state monomer of 6CN2. However, the most probable pathway for this type of aggregate structure would give rise to a modest lifetime for an aggregate, and our experimental data suggest this to be the case. Reasons for the subtlety of the aggregate optical response may be that it is either short-lived or that photoexcitation of the aggregate constituent(s) leads to dissociation. In this picture, the deprotonation of either member of the dimer would give rise to an  $\text{O}^-$  functionality in close proximity to a nucleophilic  $\text{C}\equiv\text{N}$  moiety on another 6CN2 molecule. Repulsive interactions for such a structure would force the dimer constituents apart, leaving a deprotonated  $6\text{CN}2^*$  and a protonated ground state 6CN2. This explanation for the 360 and 500 nm spectral features is

speculative, and we can gain some additional insight into its behavior using time-domain spectroscopy. Specifically, excitation of the 360 nm feature at low  $pH$  will select for the putative aggregate, and its characteristic reorientation time compared to that of monomeric 6CN2 will place limits on the lifetime of the aggregate.

*Time Domain spectroscopic results.* We have used time-correlated single photon counting measurements to characterize the timescale of protonation and deprotonation for 6CN2 and to understand the size of the species in solution. For the former experiments we have acquired “3D” fluorescence spectra, where both time- and frequency-resolved data are shown. Because the  $pK_a$  of 6CN2 is 8.4, this molecule will exist exclusively in its protonated form in the ground state at  $pH$  values less than 3. Upon excitation, because  $pK_a^* = 0.25$ , we expect efficient deprotonation, leading to a decay of the 370 nm emission feature and a corresponding build-up of the 440 nm emission band. We observe these trends experimentally (Figure 2.8), and have acquired the 3D emission spectra for 6CN2 at a series of  $pH$  values.

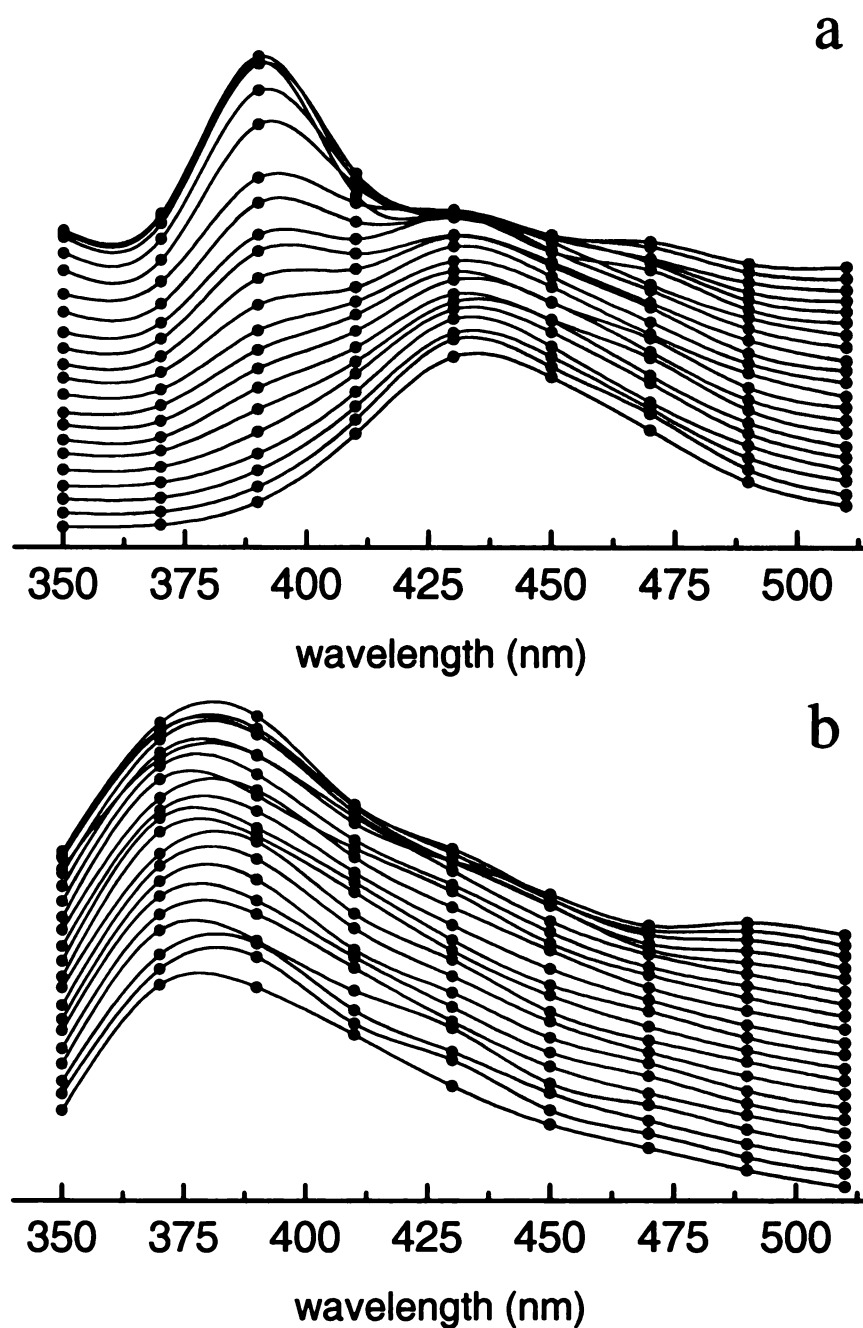


**Figure 2.8 . (a) Time resolved emission spectra of 6CN2 in 0.1 M NaOH, (b) Time resolved emission spectra of 6CN2 in 2 M HCl. For both spectral data sets the time after excitation from top to bottom scans are 0, 20 , 30, 50, 70, 90, 110, 120, 140, 160, 180, 200, 220, 240, 260, 310, 360, 410, 460 and 510 ps.**

We report the 370 nm decay and associated 440 nm rise time at each of these pHs in Table 1 and Figure 2.9. The data taken in 2 M HCl solution show a build-up in intensity at early times at both 370 nm and 440 nm. Because the pH of the 2M solution (-0.3) is lower than the  $pK_a^*$  of the excited chromophore, the majority of the excited molecules will remain protonated and the build-up could, in principle, be related to the time required for the solvent surrounding the chromophore to accommodate to the excited state dipole moment or to the time required by the chromophore to complete structural and vibrational relaxation within the  $S_1$  manifold. The ~240 ps build-up time is far too slow to be accounted for by solvent relaxation and it would be remarkable if population and structural relaxation within the 6CN2  $S_1$  manifold required this much time. We do not have sufficient data to elucidate the cause(s) of the build-up in both emission bands, but it is possible that other protonated species play a role in the optical response of 6CN2 at this low pH. The data for 0.6 M HCl and 0.001 M HCl yield the expected result that following excitation there is a rapid decay of the protonated species due to deprotonation, and a corresponding rise in the emission intensity of the deprotonated form at 440 nm. For both 0.6 M and 0.001 M HCl solutions the deprotonation time (fast 370 nm decay) is shorter than the build-up time for the deprotonated emission intensity, suggesting the presence of either an intermediate state or a measurably long (~50 – 100 ps) structural relaxation time for the system. The latter explanation is not likely because we do not resolve any spectral evolution aside from the expected bands in this time window.

**Table 1. Decay time constants and fractional contributions of the protonated and deprotonated forms of 6CN2. For both emission at 370 nm from the protonated form and emission at 440 nm from the deprotonated form, the data are of the form  $f(t) = A_1 \exp(-t/\tau_1) + A_2 \exp(-t/\tau_2)$ . The physical significance of the signs of  $A_1$  and  $A_2$  are discussed in the text.**

300 nm exc.	Emission at 370 ± 10 nm		Emission at 440 ± 10 nm	
	A (normalized)	$\tau$ (ps)	A (normalized)	$\tau$ (ps)
2 M HCl	-0.21 ± 0.02	190 ± 27		
	0.79 ± 0.02	1540 ± 4		
0.6 M HCl	0.10 ± 0.02	13 ± 1	-0.22 ± 0.02	196 ± 13
	0.90 ± 0.02	3847 ± 10	0.78 ± 0.02	3742 ± 14
0.001 M HCl	0.80 ± 0.09	127 ± 18	-0.36 ± 0.01	198 ± 7
	0.20 ± 0.09	480 ± 275	0.64 ± 0.01	6071 ± 32
350 nm exc.	Emission at 500 ± 10 nm			
	A (normalized)	$\tau$ (ps)		
2 M HCl	-0.46 ± 0.04	223 ± 26		
	0.54 ± 0.04	2321 ± 75		
0.6 M HCl	-0.59 ± 0.05	247 ± 35		
	0.41 ± 0.05	2984 ± 357		
0.001 M HCl	-0.45 ± 0.08	233 ± 29		
	0.55 ± 0.08	4343 ± 341		



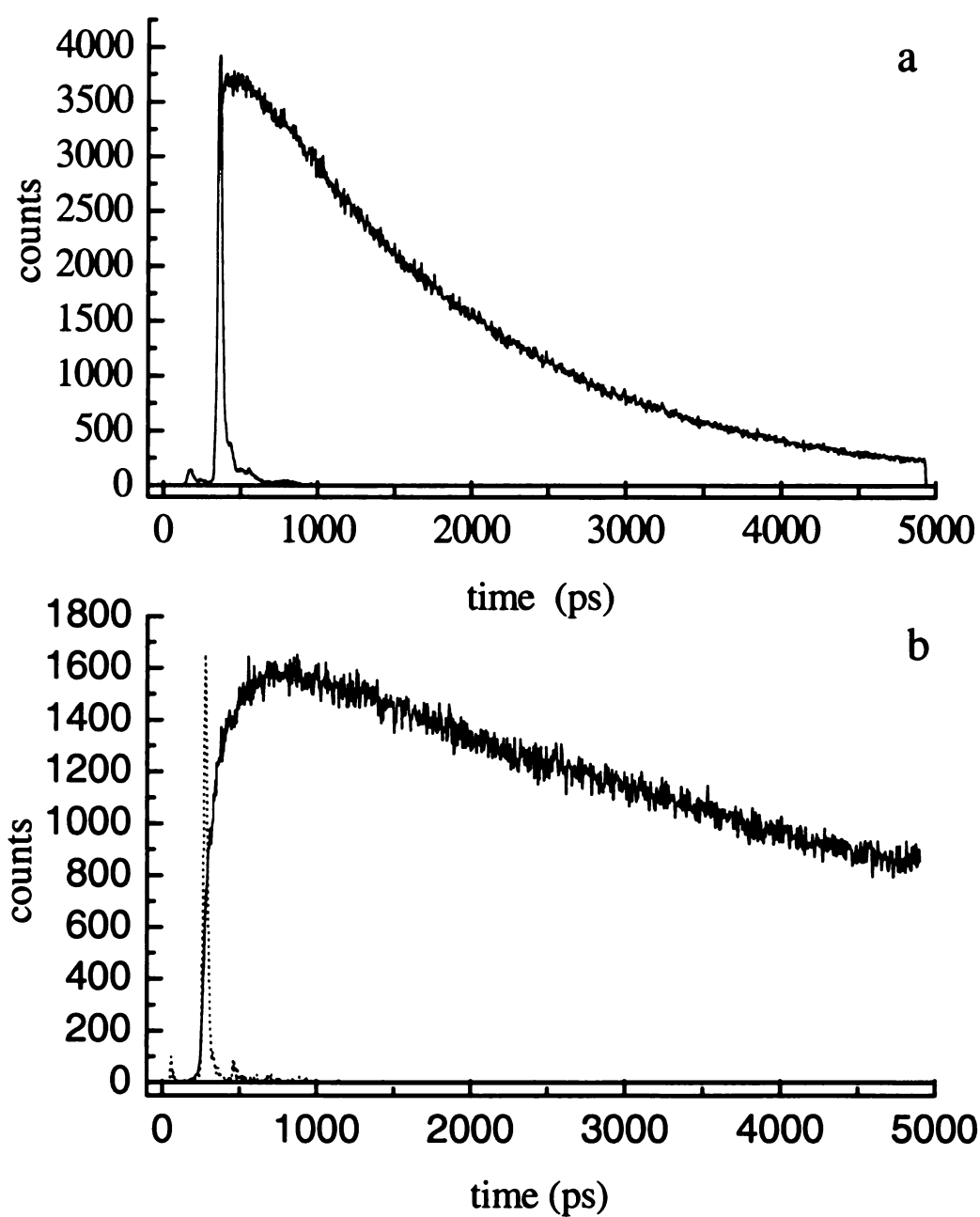


**Figure 2.9 : (a) Fluorescence lifetime of  $1 \times 10^{-5} \text{ M}$  6CN2 in 2M HCl, excited at 300 nm, emission collected at 370 nm. (b) Fluorescence lifetime of  $1 \times 10^{-5} \text{ M}$  6CN2 in  $1.0 \times 10^{-5} \text{ M}$  NaOH, excited at 300 nm, emission collected at 440 nm.**

The lifetime data exhibit a relatively  $pH$ -independent time constant for the evolution of the deprotonated form of 6CN2, which is not expected. It has been postulated that water dimers are adequate to accommodate the proton released by the 6CN2 molecule upon excitation.<sup>2</sup> Because we perform these experiments in an aqueous medium, there is a substantial excess of water molecules in the immediate vicinity of 6CN2, thereby placing the deprotonation reaction in a quasi-zeroth order regime.

We consider next the long lifetime data for excitation at 300 nm and collection of emission at 370 nm (protonated 6CN2) and 440 nm (deprotonated 6CN2). For emission at 370 nm, there is the expected  $pH$  dependence for the 2.0 M and 0.6 M HCl solutions (*vide infra*), with the long time emission behavior of the 370 nm band of 6CN2 in 0.001 M HCl being anomalously short. We ascribe this anomalous behavior to the fact that the  $pH$  of the solution is more than 3  $pH$  units above  $pK_a^*$ , so the low efficiency of geminate recombination plays a dominant role in determining the protonated 6CN2 lifetime. For emission of the 440 nm band, we recover a  $pH$  dependence that is consonant with that seen for the protonated form. The apparent  $pH$  dependence of the emission of both the 370 and 440 nm bands is likely due not to  $[H^+]$ , but to  $[Cl^-]$ . Chloride ion is an efficient quencher and a Stern-Volmer plot of the emission rate constant as a function of  $[Cl^-]$  yields a linear relationship and a quenching constant of  $K_q = 1.75 \pm 0.63 \text{ M}^{-1}$  (Figure 2.10a).<sup>21</sup> We note that the decay time constant for the protonated and deprotonated forms of 6CN2 is essentially the same for 0.6 M HCl, which corresponds to a solution where  $pH = pK_a^*$ . While it is not necessary,

and possibly not likely that  $K_q$  will be similar for the protonated and deprotonated forms of 6CN2, we note that phenomenologically, we observe  $K_q$  to be the same for both species (Figure 2.10a), suggesting the relative unimportance of ionic charge in this collisional quenching process.

The Stern-Volmer quenching analysis applied to the data assumes that collisional (dynamic), quenching is occurring due to  $\text{Cl}^-$  in solution. The quenching occurs as a result of a collisional interaction between the  $\text{Cl}^-$  and excited 6CN2. The collisional quenching rate is limited by diffusion, the efficiency of  $\text{Cl}^-$ -6CN2\* collisional relaxation, and changes in the temperatures and viscosity of the solution, which can affect the quantum efficiency.<sup>22</sup> In order to determine the quenching constant of  $\text{Cl}^-$  and 6CN2 in the solution, the  $[\text{Cl}^-]$  has to be high enough so the probability of a  $\text{Cl}^-$  - 6CN2 interaction is on the same order as the probability of a radiative relaxation event for 6CN2. The Stern-Volmer equation is

$$(\Phi_F^0 / \Phi_F) = 1 + K_q[\text{Q}] \quad (1)$$

where  $\Phi_F^0$  is the fluorescence quantum yield of 6CN2 without  $\text{Cl}^-$  present in solution,  $\Phi_F$  is the fluorescence quantum yield with  $\text{Cl}^-$  present,  $K_q$  is the Stern-Volmer quenching constant, and  $[\text{Q}]$  is the concentration of the quencher Q, which in our case is  $\text{Cl}^-$ . Upon rearrangement of this equation to solve for  $\Phi_F^{-1}$ , a plot of the reciprocal of the observed fluorescence signal of 6CN2 vs the  $[\text{Cl}^-]$  yields a straight line as demonstrated in Figure 2.10, of which the Stern-Volmer constant,  $K_q$  can be determined. The fluorescence quantum yield and the fluorescence lifetimes are one in the same. Table 2.1 reports the fluorescence

lifetime values of 6CN2 in various concentrations of HCl. Upon higher HCl concentrations, the lifetimes decrease confirming that Cl<sup>-</sup> is interacting with the 6CN2 and quenching the fluorescence of 6CN2 contributing to different lifetime values.

We have also measured the lifetime of the 500 nm band after excitation at 350 nm. Our data show two important trends. The first is that the 500 nm emission transients at all *pH*s are characterized by a ~230 ps build-up time. As discussed above, the origin of this rise-time remains to be resolved unambiguously, but for the aggregate such a transient response would be consistent with the formation of an exciplex. The presence of the 350 nm absorption band at low *pH* demonstrates the existence of ground state aggregate, but excitation of this species may be associated with a structural realignment to an emissive state. The second significant feature of these data is the *pH* dependence of the long emission lifetime. These long time decays are consistent with collisional quenching by Cl<sup>-</sup> and when the same Stern-Volmer treatment is applied to these data, we recover a linear dependence with a  $K_q = 0.43 \pm 0.07 \text{ M}^{-1}$  (Figure 2.10b). The fact that the  $K_q$  is smaller for the aggregate than for either protonated or deprotonated 6CN2 demonstrates that the aggregate is structurally distinct from the monomeric forms. With this information in hand, it is instructive to consider the motional dynamics of both the monomeric and aggregate species.

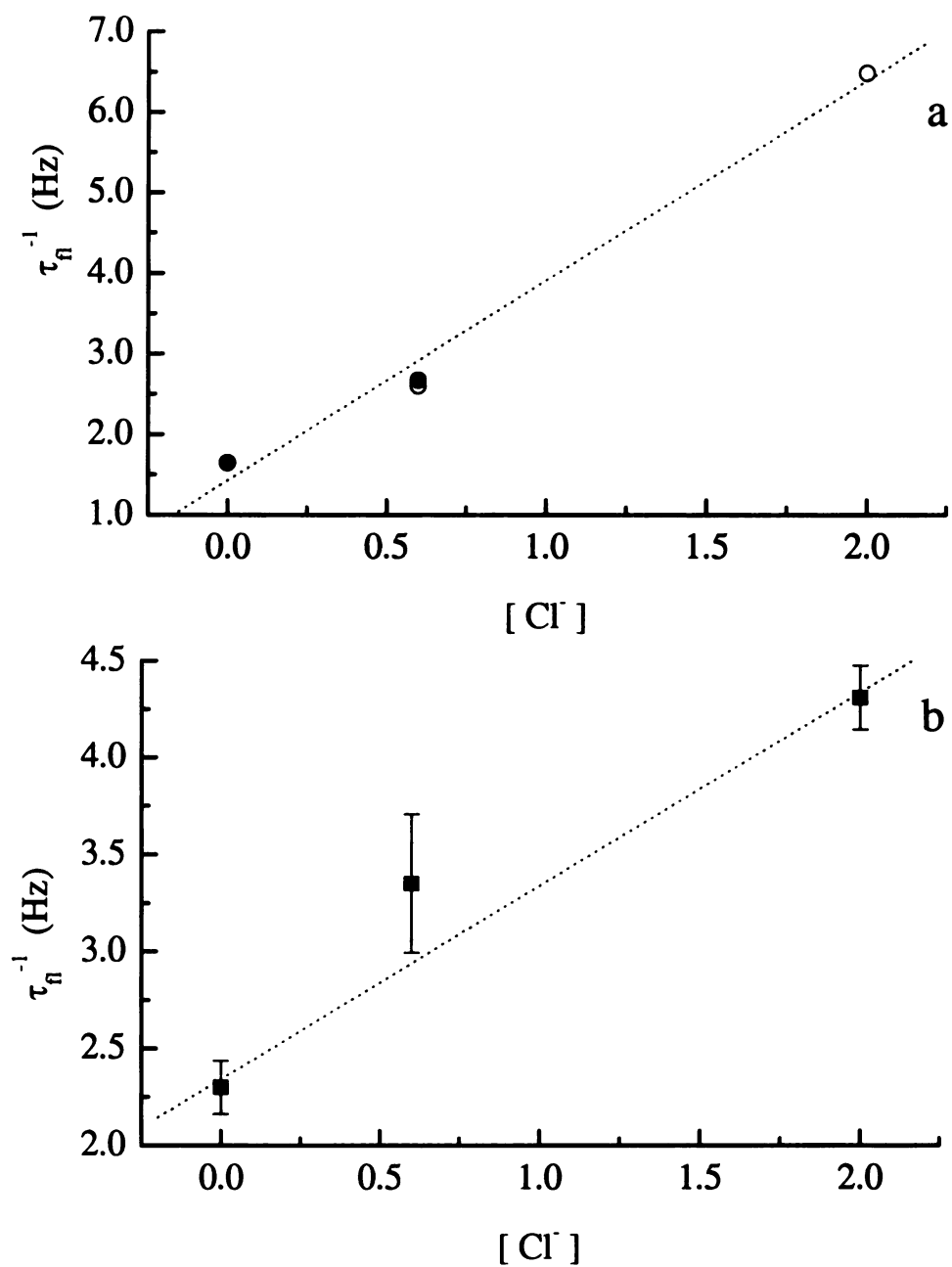


**Figure 2.10:** (a) Stern-Volmer plot for the protonated form of 6CN2 (o) and the deprotonated form of 6CN2 (•) quenched by  $\text{Cl}^-$ . Lifetimes for the protonated form were acquired at 370 nm and 440 nm for the deprotonated form. (b) Stern-Volmer plot of quenching of the aggregate species by  $\text{Cl}^-$ . Data were acquired using 350 nm excitation and 500 nm emission.

When probing the existence of the dimer at excitation 350 nm, very basic solutions had similar results to excitation at 300 nm and this agrees with our steady state spectra, since there should be no dimer present at *pH*s higher than 3. When looking at the “3D” spectral profile of 0.6 M HCl, Figure 2.11, one notices there is a sharp peak around 420 nm with a rapid decay also with a small, yet noticeable rising peak at 500 nm. This particular 3D spectrum is noisy compared to any obtained at excitation 300 nm and this is because the fluorescence intensity probing at 350 nm for low *pH* solutions is extremely low. There is a considerable amount of more noise present.

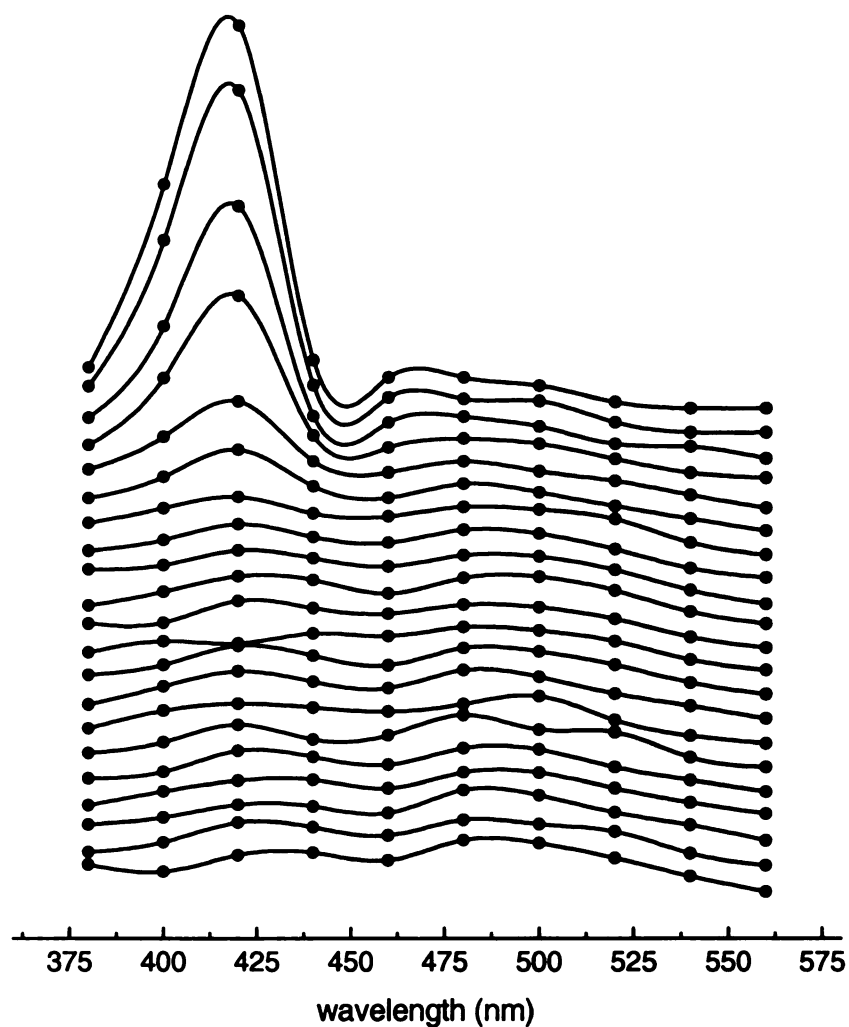


**Figure 2.11 : Time Resolved spectra of 6CN2 in pH = 0.25 (0.6 M HCl), during the first 500 ps of the molecule's lifetime. Peak maximum at first is at 420nm and dies down. There is a faint trace of peak at 500nm. The time after excitation from top to bottom scans are 0, 20 , 30, 50, 70, 90, 110, 120, 140, 160, 180, 200, 220, 240, 260, 310, 360, 410, 460 and 510 ps.**

To see the raw data, that was not altered, one can see a short lifetime of the 420 nm emission, Figure 2.12a, and a long component of a peak at 500 nm emission, Figure 2.12b. When comparing all acid solutions of 6CN2 and the

steady state spectrum (Figure 2.6), it can be concluded that the 500 nm peak shifts to shorter wavelengths upon raising the  $pH$ , and the 420 nm peak increases in intensity and moves to longer wavelengths at the same time. This suggests that the dimer is present but very short-lived, which is confirmed by our time-domain data with the noise in the spectra. The 420 nm peak that is small at very acidic concentrations but increases in intensity and broadness upon more basic solutions is actually showing that there is a small amount of the excited state deprotonated monomer present.



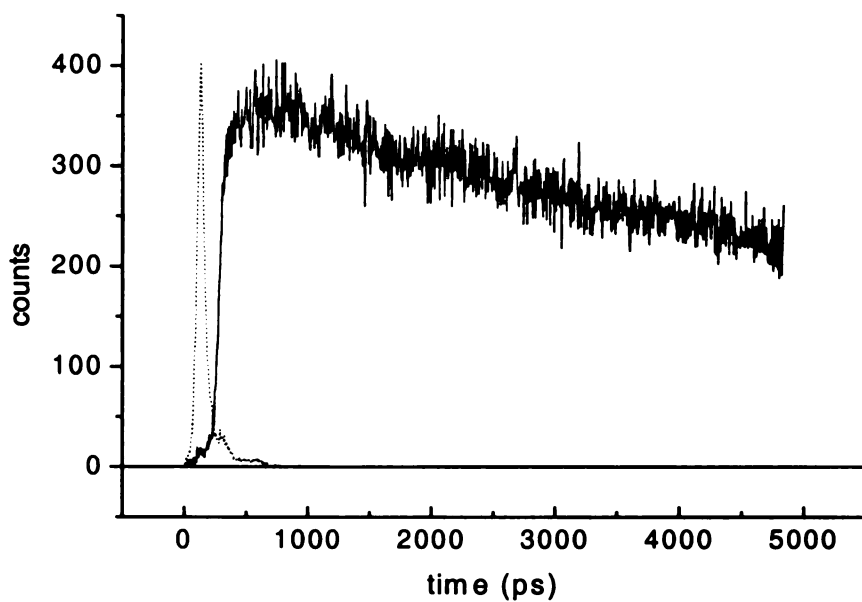
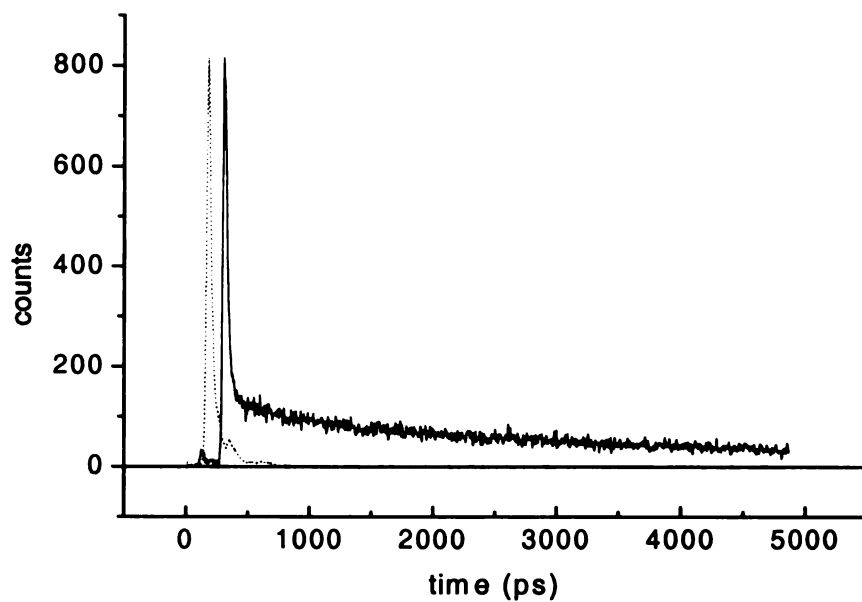


**Figure 2.12 (a) Fluorescence lifetime of  $1 \times 10^{-5} \text{ M}$  6CN2 in 0.6M HCl, excited at 350 nm, emission collected at 420 nm. (b) Fluorescence lifetime of  $1 \times 10^{-5} \text{ M}$  6CN2 in 0.6M HCL, excited at 350 nm, emission collected at 500 nm.**

The lifetime data exhibit a relatively *pH*-independent protonation and deprotonation time constant, which is surprising (Table 1). Several models have been developed to account for proton transfer to the solvent and for many photoacids it has been postulated that between two and four water molecules are required to accommodate the proton released by the 6CN2 molecule upon excitation. Robinson<sup>20</sup> developed some of these theories, especially with 2-naphthols. These theories are especially applied to weak photoacids, in other words photoacids that do not have a large *pH* jump. However, because 6CN2 is a super photoacid, the water dimers, if formed are effective proton acceptors because solvent reorganization is less critical for proton to solvent transfer<sup>2</sup>. Because we perform these experiments in aqueous medium, it is likely that there is a substantial excess of water molecules in the immediate vicinity of 6CN2, thereby placing the deprotonation reaction in a quasi-zeroth order regime.

We have measured the reorientation times of 6CN2 in several environments, and present these data in Table 2. The reorientation information is extracted from fluorescence intensity decays polarized parallel and perpendicular to the vertical excitation polarization. These experimental intensity data are used to generate the induced orientational anisotropy function,  $R(t)$ ,

$$R(t) = (I(t)_{\parallel} - I(t)_{\perp}) / (I(t)_{\parallel} + 2I(t)_{\perp}) \quad (2)$$

The function  $R(t)$  decays with up to five exponential components, but the most common form is to observe a single exponential decay. Experimentally, two decays are seen at most, and the resolution of multiple decay components is based to a significant extent on the inherent symmetry of the reorienting molecule and any restrictions the local environment places on the motion of the chromophore. Owing to the low symmetry of 6CN2 and the low viscosity of the aqueous solutions we report on here, we would expect this chromophore to exhibit a single exponential decay anisotropy.

**Table 2. Reorientation time(s) for 6CN2 as a function of pH and at different excitation and emission wavelengths. In cases where multiple components of the anisotropy decay are seen, we ascribe each decay component to an individual species.**

300 nm exc.	370 nm emission		440 nm emission		500 nm emission	
	R(0)	$\tau_{OR}$ (ps)	R(0)	$\tau_{OR}$ (ps)	R(0)	$\tau_{OR}$ (ps)
2 M HCl	$0.40 \pm 0.10$	$207 \pm 21$	$0.18 \pm 0.02$	$179 \pm 25$	$0.26 \pm 0.08$	$167 \pm 38$
0.6 M HCl	$0.18 \pm 0.04$	$224 \pm 71$	$0.13 \pm 0.06$	$208 \pm 29$		
$1.0 \times 10^{-5}$ M NaOH			$0.19 \pm 0.05$	$123 \pm 23$		
350 nm exc.						
2 M HCl					$0.31 \pm 0.04$	$159 \pm 35$
0.6 M HCl					$0.22 \pm 0.12$	$135 \pm 58$
$1.0 \times 10^{-5}$ M NaOH						

To interpret the reorientation times we use the modified Debye-Stokes-Einstein (DSE) model,<sup>20-21,23</sup> where the time constant of the anisotropy decay is related to the hydrodynamic volume (V) and shape (S) of the reorienting moiety and the temperature (T) and viscosity ( $\eta$ ) of the solvent medium.

$$\tau_{OR} = \frac{\eta Vf}{k_B TS} \quad (3)$$

For 6CN2 the hydrodynamic volume is 151 Å<sup>3</sup>,<sup>24</sup> we take the solution viscosity to be 1 cP for all systems studied here,  $f$  = the solvent-solute friction coefficient, which is 1 in water,  $k_B$  is the Boltzmann constant and  $T = 300$  K. We assume the solute shape factor to be unity (spherical solute) because the reorientation data do not provide sufficient information to allow modeling this quantity accurately. The DSE model assumes the solvent to be a continuum and is thus limited by its inability to account for molecular interactions explicitly. Despite this limitation, the modified DSE model is capable of predicting the reorientation behavior of polar solutes in polar solvents with remarkable accuracy. Using Eq. 3, we estimate  $\tau_{OR} = 50$  ps for 6CN2 in water. We note that the DSE model significantly underestimates the measured reorientation times for both protonated and deprotonated 6CN2 in water. For excitation at 300 nm, we recover a reorientation time constant of ca. 200 ps in all cases, with the time constant for the basic form being the smallest ( $123 \pm 23$  ps) by a substantial amount. Such “super stick” behavior has been observed before for polar dyes in protic solvents, but it is interesting to note here that both the neutral and anionic forms of 6CN2 are characterized by the same reorientation time to within the experimental uncertainty, suggesting rapid proton exchange in this system. We note that

super photoacids are thought to exist within an extensive H-bonded network formed between the solute and the solvent.<sup>2</sup> If this is the case, the reorienting moiety would be significantly larger than the bare 6CN2 molecule, consistent with these data.

For excitation of 6CN2 at 350 nm, only the 500 nm emission data yield useful reorientation information, and this is expected based on the spectral profiles of the monomer and aggregate species. We find that for 350 nm excitation and 500 nm emission, the aggregated species reorients with the same time constant as the monomer species, despite being characterized by a substantially different Stern-Volmer quenching constant. The fact that the aggregate exhibits a ca. 150 ps reorientation time suggests that either the lifetime of the aggregate is on the order of the reorientation time, or the solvated reorienting moiety is substantially the same in size as that of the solvated monomer species. Because of the pH dependence of the long lifetime of the excimer species it is not physically reasonable to conclude that the lifetime of the aggregate is on the order of hundreds of ps. The fact that the reorientation time of both the monomeric and aggregate species lies in the “super stick” regime indicates that the reorienting moiety, *i.e.* the solute(s) and some amount of solvent, is not substantially different in any of these cases. Based on the DSE model, the monomer hydrodynamic volume of 150 Å<sup>3</sup> is consistent with a reorientation time of 50 ps, as indicated above. The experimental reorientation time of 150 – 200 ps observed experimentally suggests a reorienting moiety of 450 – 600 Å<sup>3</sup> in the limit of a “sticky” solvent-solute boundary condition. Since

the 450 – 600 Å<sup>3</sup> volume is substantially larger than either the monomer or a putative dimeric species, we are not able to discern detailed information on the aggregated species in solution, other than to say that its lifetime is on the order of four ns or more based on the fluorescence lifetime data.

The steady state and time-resolved spectroscopic data on the excitation of 6CN2 at 300 nm indicate that it behaves primarily as a monomeric species in solution. Our data for  $pK_a^*$  are in agreement with other literature reports<sup>1,12,15</sup> and our lifetime data show that protonation and deprotonation operates on the ~100 ps timescale, nominally independent of  $pH$  over a substantial range. When 6CN2 solutions at low  $pH$  are excited at 350 nm, we find evidence for a new species in solution. The ca. 350 nm absorption band is associated with an emission band at 500 nm, and the intensity of these features relative to those of the 6CN2 monomer increases with decreasing  $pH$ . These data collectively reveal a complex dynamical system which we have schematized in Figure 2.13. As is well established, the ground state and excited state protonation and deprotonation dynamics are governed by substantially different equilibrium constants, which are themselves the result of state-dependent changes in the  $\pi$ -electron density distribution in the 6CN2 chromophore. These equilibria are well characterized, but the equilibrium between monomeric and aggregated forms of 6CN2 is somewhat less well determined. Our data indicate that the aggregate is present to a significant extent only in solutions with  $pH \leq pK_a^*$ , and that the lifetime of the aggregate is on the order of nanoseconds. The fact that we observe the aggregate in the excitation spectrum indicates that the initial

complexation occurs in the ground state, consistent with the higher propensity of ground state 6CN2 to retain its proton and thus remain neutral. We do not know the extinction coefficient for the ca. 350 nm absorption band associated with the aggregate, so it is not possible to readily estimate the value of the formation constant for the aggregate. The fact that we monitored the presence of the aggregate by emission spectroscopy accounts for the observation that the aggregate is readily seen for  $pH \leq pK_a^*$ . Once the aggregate is excited, its lifetime is at least as long as its fluorescence lifetime, several nanoseconds, and the complex is susceptible to collisional quenching as seen by the Stern-Volmer dependence of aggregate lifetime on  $[Cl^-]$ . Reorientation data do not shed light on the size of the complex directly, but all reorientation measurements indicate that the reorienting moiety is substantially larger than the chromophore alone. Thus, our frequency- and time-domain data on the aggregate provide limited information on the structural details of the aggregate. Despite these limitations, however, the clear demonstration of an aggregate of 6CN2 provides support for an entity that has been hinted at in the literature for several years.<sup>7,12</sup>

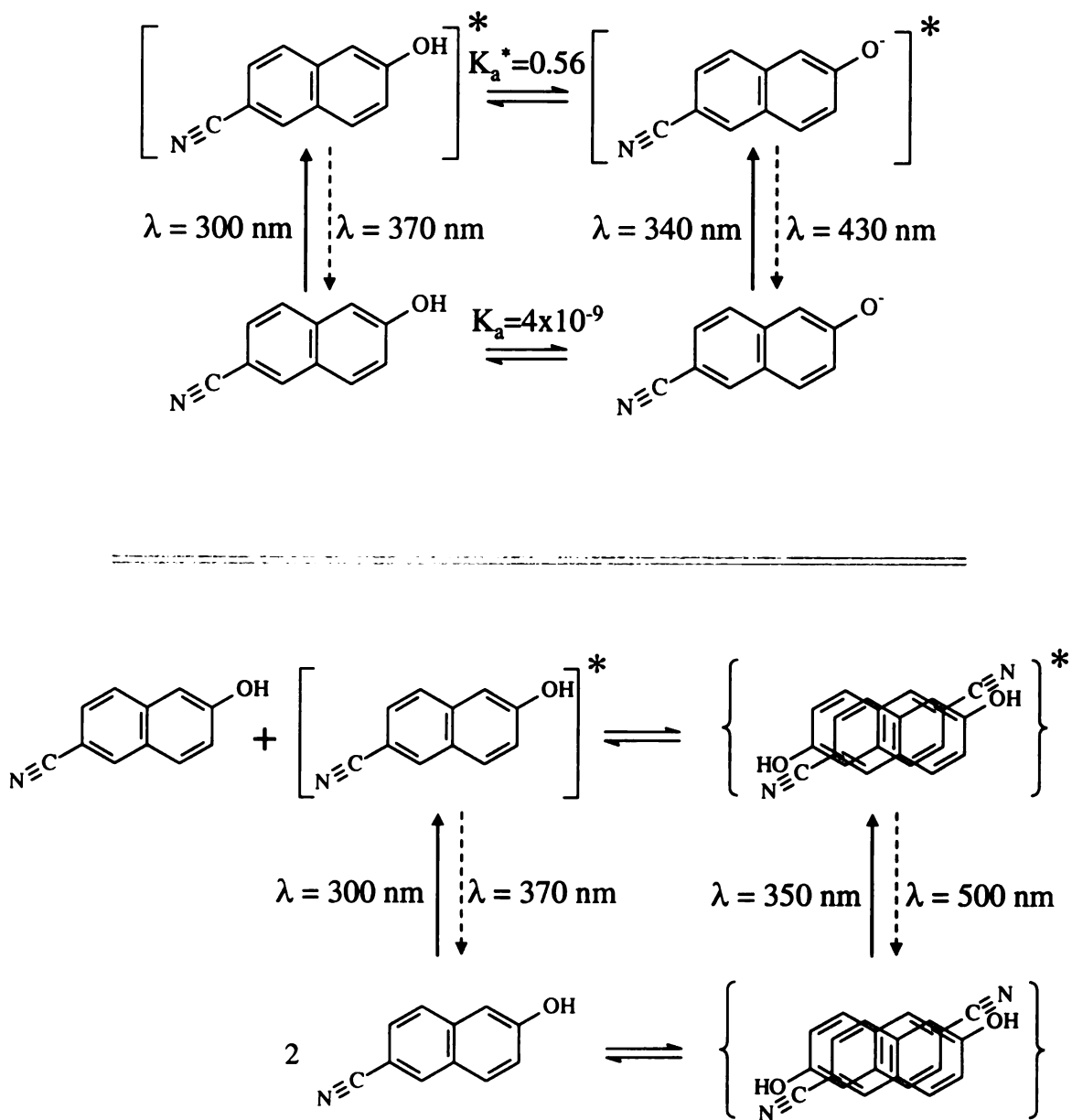


**Figure 2.13: 6CN2 equilibria relevant to this work. Top pane: Protonation/deprotonation equilibria with ground state and excited state  $K_a$ 's indicated. Absorption and emission maxima are indicated. Bottom pane: Proposed aggregation equilibria. We have implied the identity of the aggregate species to be a dimer for reasons of physical and chemical plausibility (see text).**



## 2.4 Conclusions

We have examined the time- and frequency-domain optical properties of the photoacid 6CN2 in an effort to understand the dynamics of this chromophore and its potential utility for effecting transient *pH* changes in solution. Our determination of  $pK_a^* = 0.25$  is in agreement with previous literature reports for this compound and the time-domain spectra demonstrate the temporal evolution of the protonated and deprotonated forms of the chromophore subsequent to excitation. We account for the functional forms of the spectroscopic transients in the context of protonation/deprotonation and collisional quenching by  $Cl^-$  ions. Excitation spectra reveal the presence of an aggregate characterized by an absorption band centered at ca. 350 nm and an emission band centered near 500 nm. The emission of this aggregated species is quenched collisionally by  $Cl^-$  with a Stern-Volmer quenching constant different than that of either the neutral or anionic 6CN2 monomer. Time-domain fluorescence depolarization measurements show the aggregate species to reorient with the same diffusion constant as the monomer to within the experimental uncertainty. The recovered time constants for all species are longer than those expected based on the modified Debye-Stokes-Einstein model, making reorientation measurements less useful than anticipated. These data, taken collectively, demonstrate the existence of a transient aggregate of 6CN2 in solution, with the likely dissociation of the excited aggregate being determined by deprotonation of one of the aggregate substituents.

## 2.5 Literature Cited

1. Tolbert, L. M.; Haubrich, J. E. *J. Am. Chem. Soc.*, **1990**, *112*, 8163.
2. Tolbert, L. M.; Haubrich, J. E. *J. Am. Chem. Soc.*, **1994**, *116*, 10593.
3. Huppert, D.; Tolbert, L. M.; Linares-Samaniego, S. *J. Phys. Chem. A*, **1997**, *101*, 4602.
4. Solntsev, K. M.; Huppert, D.; Tolbert, L. M.; Agmon, N. *J. Am. Chem. Soc.*, **1998**, *120*, 7981.
5. Solntsev, K. M.; Huppert, D.; Agmon, N. *J. Phys. Chem. A*, **1999**, *103*, 6984.
6. Cohen, B.; Huppert, D. *J. Phys. Chem. A*, **2000**, *104*, 2663.
7. Solntsev, K. M.; Huppert, D.; Agmon, N.; Tolbert, L. M. *J. Phys. Chem. A*, **2000**, *104*, 4658.
8. Solntsev, K. M.; Agmon, N. *Chem. Phys. Lett.*, **2000**, *320*, 262.
9. Knochenmuss, R.; Solntsev, K. M.; Tolbert, L. M. *J. Phys. Chem. A*, **2001**, *105*, 6393.
10. Agmon, N.; Rettig, W.; Groth, C. *J. Am. Chem. Soc.*, **2002**, *124*, 1089.
11. Barroso, M.; Arnaut, L. G.; Formosinho, S. J. *J. Photochem. Photobio. A*, **2002**, *154*, 13.
12. Clower, C.; Solntsev, K. M.; Kowalik, J.; Tolbert, L. M.; Huppert, D. *J. Phys. Chem. A*, **2002**, *106*, 3114.
13. Cohen, B.; Segal, J.; Huppert, D. *J. Phys. Chem. A*, **2002**, *106*, 7462.
14. Solntsev, K. M.; Tolbert, L. M.; Cohen, B.; Huppert, D.; Hayashi, Y.; Feldman, Y. *J. Am. Chem. Soc.*, **2002**, *124*, 9046.
15. Tolbert, L. M.; Solntsev, K. M. *Acc. Chem. Res.*, **2002**, *35*, 19.
16. DeWitt, L.; Blanchard, G. J.; LeGoff, E.; Benz, M. E.; Liao, J. H.; Kanatzidis, M. G. *J. Am. Chem. Soc.*, **1993**, *115*, 12158.

17. Schulman, S. G. Acid Base Chemistry of Excited Singlet States. In *Modern Fluorescence Spectroscopy*, Wehry, E. L., Ed.; Plenum Press: New York, 1976; pp 239.
18. Ingle, J. D.; Crouch, S. R. *Spectrochemical Analysis*; Prentice Hall: Upper Saddle River, NJ, 1988.
19. Robinson, G.W. *J. Phys. Chem.*, **1991**, *95*, 10386
20. Debye, P. *Polar Molecules* Chemical Catalog Co.: New York 1929.
21. Szabo, A. *J. Chem. Phys.*, **1984**, *81*, 150.
22. Ingle, J.D. and Crouch, S.R. *Spectrochemical Analysis* Prentice Hall, New Jersey **1988**
23. Perrin, F. *J. Phys. Radium*, **1934** *5*, 497.
24. Edward, J. T. *J. Chem. Ed.*, **1970**, *47*, 261.

## Chapter 3

### Using the Photoacid 6CN2 with a Weak Acid System

#### Summary

We report on the complexation between adipic acid and 6-cyano-2-naphthol (6CN2) in aqueous solution. Adipic acid ( $H_2AA$ ) is a diprotic weak acid which has a  $pH$  dependent solubility in an aqueous solution. The solution is buffered slightly above  $pH=4.4$ , close to  $pK_{a1}$  for adipic acid. The goal is to poise the system to contain enough hydrogen-adipate anions ( $HAA^-$ ) that if protonated, would produce a supersaturated  $H_2AA$  concentration. The photoacid 6CN2 is used to donate protons to this solution upon excitation. We investigate the spectroscopic properties of 6CN2 in this buffered system using steady state spectroscopy and time correlated single photon counting (TCSPC).

### 3.1 Introduction

Many industries utilize crystallization as a method of production, purification, or even to recover solid starting materials. Crystallization methods can result in a product that is a large crystal or an amorphous solid with little control over is the key factors that determine the size of the crystals.<sup>1-8</sup> The larger the particle the more techniques can be applied to determine the actual molecular structure of the product and other properties of the crystal. The mechanical, electrical, magnetic, and optical properties of a material can vary according to the crystal size, habit, and packing of its constituent molecules. In general, it is commonly considered the more crystalline a product, the higher its purity. Many commercially mass produced products depend upon the pure starting materials to produce useful product.<sup>1</sup> An example of a commercial product whose production output is dependent upon the purity of its starting materials is nylon 6, 6<sup>9</sup>.

Nylon 6, 6 is a widely used polymer that is made from a reaction of adipic acid and 1, 6-hexane diamine. The purity of nylon 6, 6 can be limited by the purity of the adipic acid used. Adipic acid is rarely found in nature, and it is synthetically produced in a variety of ways, with most of them starting with reactants involving the oxidation of cyclohexane into cyclohexanol and cyclohexanone<sup>10-12</sup>. During this synthesis the products are then reacted with nitric acid, resulting in the production  $\text{NO}_2 (g)$

Adipic acid is a polyprotic acid that has two  $pK_a$ 's, and the crystallization event happens is below the first  $pK_a$ . Investigations into the early events of pH

dependence of crystallization have been explored.<sup>13-18</sup> Ideally the  $\text{H}_2\text{AA}$  solution is buffered to a  $\text{pH}$  near the  $\text{pK}_{\text{a}1}$  using  $\text{HAA}^-$  ready to accept a proton and precipitate the  $\text{H}_2\text{AA}$  out of solution. Significant control over  $\text{pH}$  in a buffered system is difficult, so the buffer constituent concentrations should be established with an eye toward minimum buffer capacity. This condition may or may not be consistent with poisoning the system near its solubility limit. Figure 3.1 shows the equilibria adipic acid undergoes.

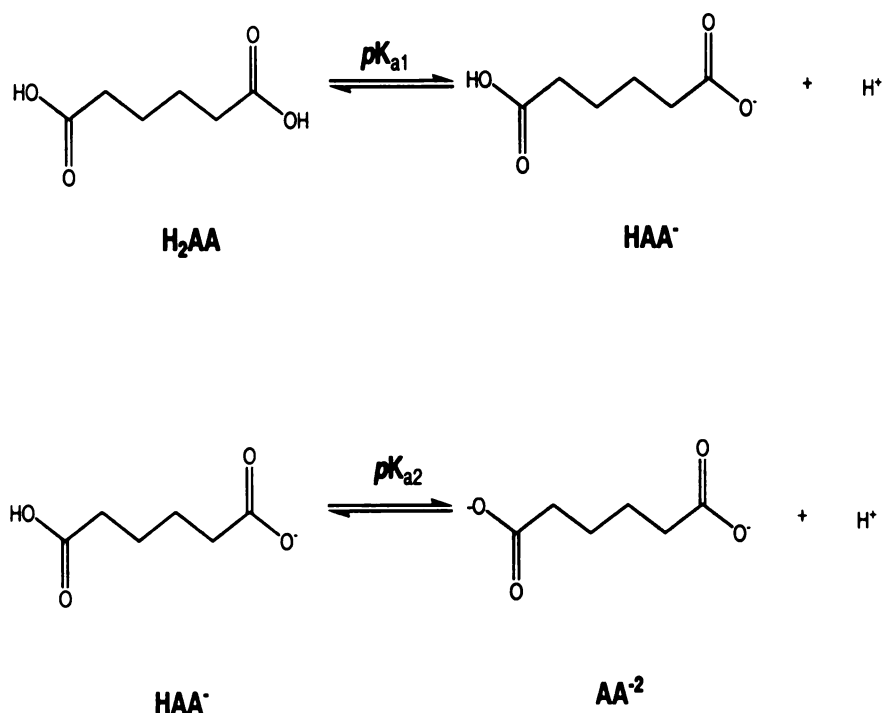


**Figure 3.1:** Adipic acid ( $\text{H}_2\text{AA}$ ) and adipate anion ( $\text{AA}^{2-}$ ) and hydrogen adipate anion ( $\text{HAA}^-$ ) equilibrium.<sup>19</sup> The first  $\text{pK}_{\text{a}} = 4.4$  and the second  $\text{pK}_{\text{a}} = 5.4$ .

One means of controlling the  $\text{pH}$  of the solution is through the use of a photoacid. In this case we use the photoacid 6CN2 to control the  $\text{pH}$  in the

adipic acid solution. The spectroscopic properties of 6CN2 were reported in Chapter 2 of this thesis. By knowing the spectroscopic properties of 6CN2 we will see how the properties change upon being in a buffered solution containing  $\text{HAA}^-$  and  $\text{H}_2\text{AA}$ . The solutions used here will contain enough  $\text{HAA}^-$  anions so that upon protonation, a supersaturated concentration of  $\text{H}_2\text{AA}$  can be created. The photoexcitation of 6CN2 will ideally induce a local  $\text{pH}$  drop sufficient to induce crystallization of  $\text{H}_2\text{AA}$  if the concentrations of  $\text{HAA}^-$ , 6CN2, and  $\text{H}_2\text{AA}$  are set appropriately. This chapter reports on our initial steps in evaluating the feasibility of this means of crystallization.

A laser is used to excite the 6CN2 and in the path of the light, protons are donated by the excited 6CN2 to its local environment. The disassociated proton could associate with the solvent, water, or  $\text{H}_2\text{AA}$  or it could recombine with the 6CN2 anion. We have demonstrated that there is an associative interaction between the buffered adipic acid system and the photoacid, which we can describe in the context of dipolar and hydrogen bonding interactions. We will also investigate the steady state and time domain spectroscopic properties of 6CN2 in the presence of adipic acid.

## 3.2 Experimental

*Chemicals.* 6CN2 was obtained from TCI America and adipic acid and sodium adipate were obtained from Aldrich (both 99% purity). All chemicals were used as received and no further purification was done. All solutions were made with deionized water. Various concentrations of sodium adipate and adipic acid were used and mixed together. The solution was constantly stirred and heated until all solids were dissolved. Then the solution was slowly cooled to ensure adipic acid would not precipitate. If any precipitate formed, the solution was filtered and 6CN2 was added. The concentration of the 6CN2 was  $1.0 \times 10^{-5}$  M to minimize incorporation of the photoacid serving as an impurity or nucleation sites for the crystallization of H<sub>2</sub>AA. We note that this concentration of 6CN2 is good for spectroscopic purposes but may be too low to induce H<sub>2</sub>AA crystallization.

*Steady state spectroscopy.* Absorption measurements were made using a Varian Cary model 300 double beam UV-visible absorption spectrometer. All measurements were made with 1 nm resolution. Emission spectra were recorded using a JY-Spex Fluorolog 3 emission spectrometer. For all emission measurements, the excitation bandwidth was 2 nm and the emission bandwidth was 2 nm. The excitation wavelengths were 300 nm and 360 nm.

*Time-Correlated Single Photon Counting (TCSPC) Spectrometer.* The spectrometer we used for the lifetime and dynamical measurements is similar to one that has been described in detail before<sup>20</sup> and in Chapter 2. Fluorescence was collected at polarizations of 0°, 54.7°, and 90° with respect to the vertically polarized excitation pulse. The instrument response function for this system is

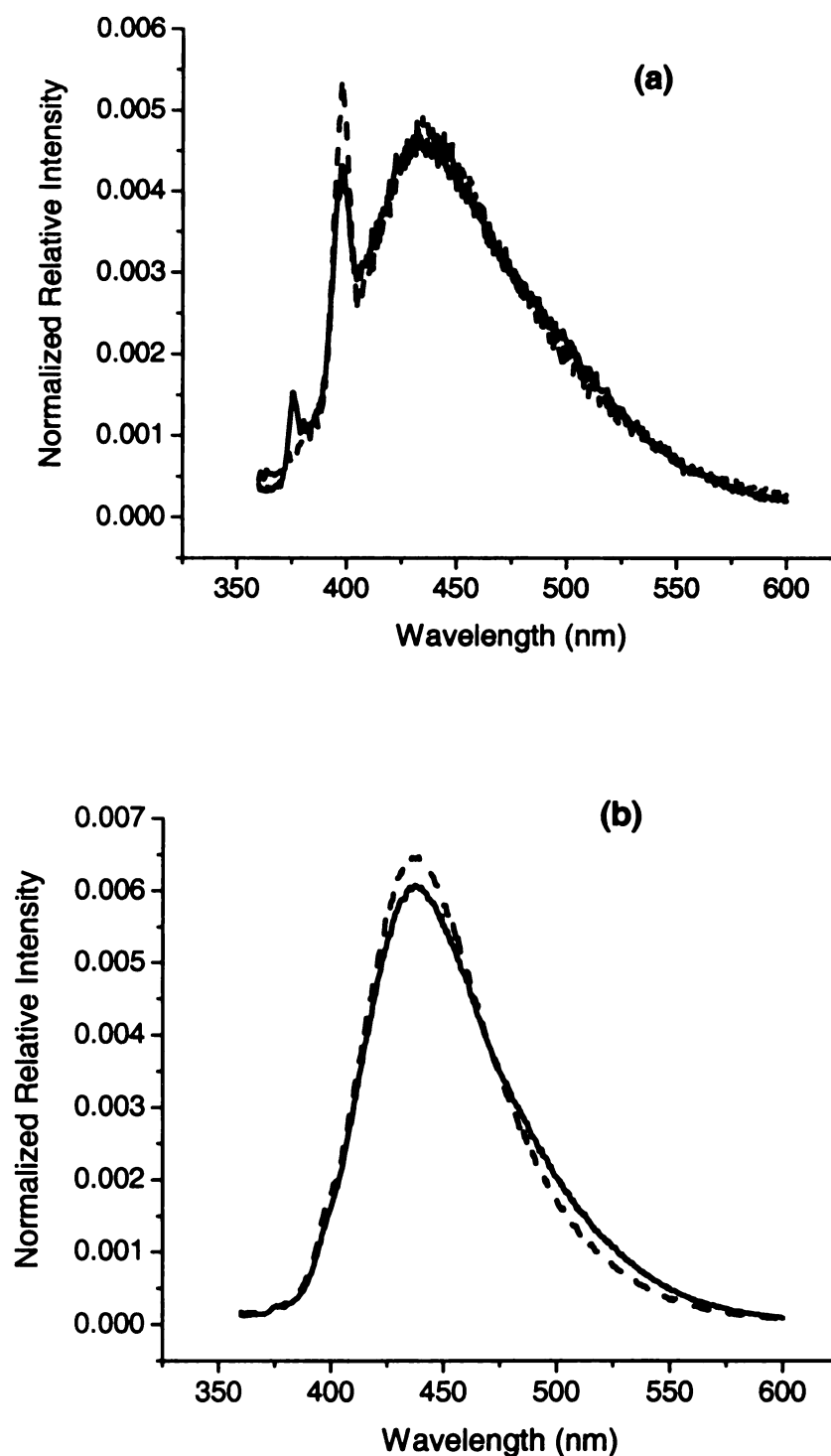


typically 35 ps FWHM and lifetimes measured range from ~100 ps to ~6 ns. We did not deconvolute the instrument response function from the experimental data. The shortest reorientation times we measure are on the order of 50 ps, and because we can recover the entire anisotropy decay, loss of the initial portion of the decay does not affect the accuracy of our determinations. The solution was also stirred with a small magnetic stir bar inside the quartz cuvette to ensure that there would be no photodegradation.

### 3.3 Results and Discussion

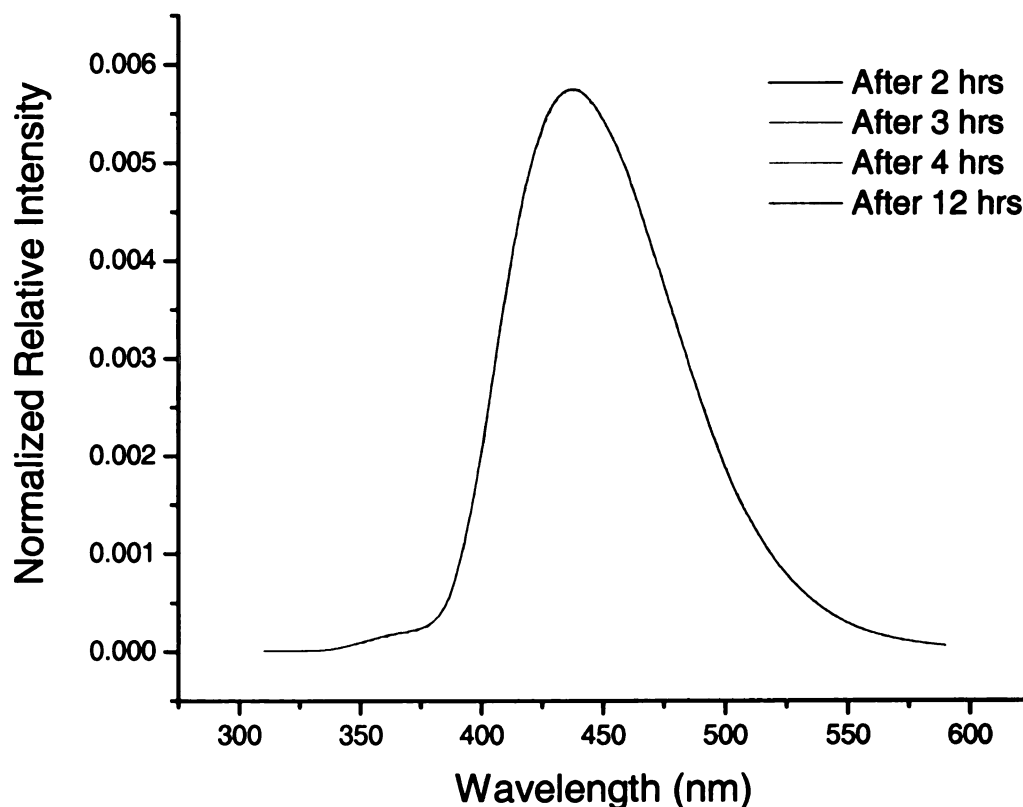
The purpose of this chapter is to explore the feasibility of 6CN2 to be crystallization initiator for H<sub>2</sub>AA. Na<sub>2</sub>AA was added to a solution of H<sub>2</sub>AA and HAA<sup>-</sup> was formed by disproportionation. Na<sub>2</sub>AA is easily dissolved in aqueous solutions to produce Na<sup>+</sup> and AA<sup>2-</sup> ions. The Na<sub>2</sub>AA is much more soluble than H<sub>2</sub>AA, which has 1.1 wt% solubility in water. The HAA<sup>-</sup> is able to accept a proton from an external proton donor such as super photoacid 6CN2. Upon protonation, H<sub>2</sub>AA is formed and possibly starting a point to start a nucleation site and facilitate crystallization growth. For samples that had H<sub>2</sub>AA and Na<sub>2</sub>AA in a 30:1 molar ratio, [H<sub>2</sub>AA] = 0.157 M and [Na<sub>2</sub>AA] = 5.17 x 10<sup>-3</sup> M. For samples that had a 10:1 ratio of H<sub>2</sub>AA/Na<sub>2</sub>AA, the concentrations were [H<sub>2</sub>AA] = 0.110 M and [Na<sub>2</sub>AA] = 9.64 x 10<sup>-3</sup> M. Samples with no Na<sub>2</sub>AA present had 0.242 M for H<sub>2</sub>AA. All solutions considered for the different ratio amounts were made in 100 mL solutions.

*Steady state spectroscopy.* Samples exposed to light were placed in a quartz cuvette and were irradiated by ultraviolet lamp over a time span of 2 to 12 hours. Steady state emission spectra were excited at two different wavelengths, 300 nm and 360 nm, before and after ultraviolet exposure. All spectra were normalized to have an integrated area equal to one to allow facile comparison between samples. No fluorescence impurities were found in buffered  $\text{H}_2\text{AA}/\text{HAA}^-$  solutions without 6CN2 present. Figure 3.2a shows that if no 6CN2 is present before and after ultraviolet lamp exposure there are no major spectroscopic changes in the buffered  $\text{H}_2\text{AA}/\text{HAA}^-$  system. The sharp peak found at 400 nm (for 300 nm excitation) is the second overtone of the Raman spectrum of water. Figure 3.2a had no 6CN2 added to the system and is normalized however when looking at the unnormalized spectrum, the fluorescence intensity of this solution is negligible compared to the fluorescence intensity of the same solution with the 6CN2. It is important to note that when the two samples are analyzed and normalized, it appears that there could be 6CN2 present in the system. A possible cause for this is that the cuvette, even though it was washed thoroughly, had minor traces of the fluorescing species present and probably sticking to the side of the cuvette. 6CN2 therefore the only fluorescing species and it is a good probe to use with the buffered solution. In a buffered  $\text{H}_2\text{AA}/\text{HAA}^-$  sample with 6CN2 present and the same exposure conditions results in a noticeable 440 nm emission peak, corresponding to the deprotonated monomer anion of 6CN2. This peak increases in intensity after constant exposure to the ultraviolet lamp (Figure 3.2b).



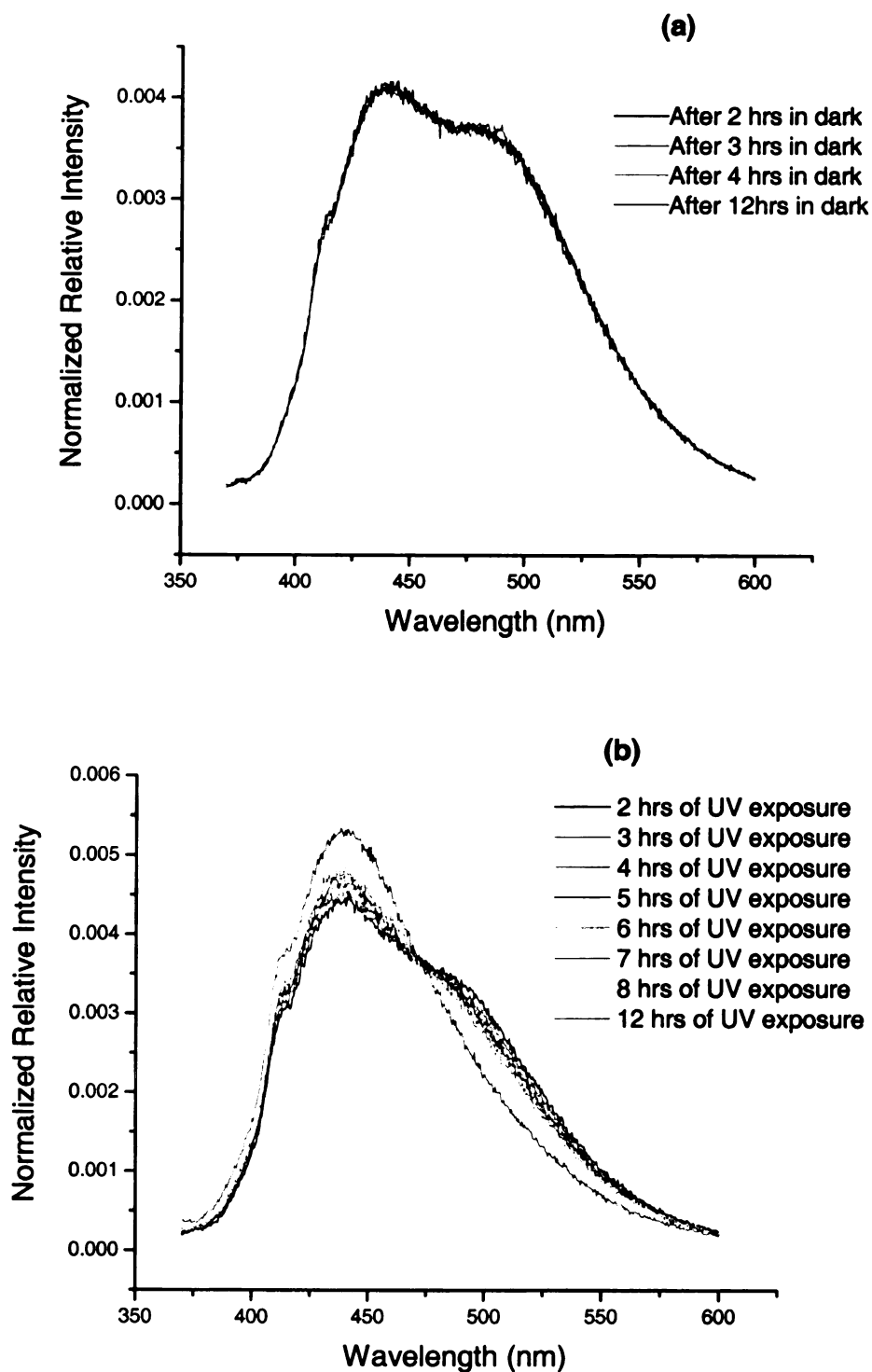
**Figure 3.2: Steady state spectra of samples for excitation at 300 nm, solid line is spectrum taken prior to UV exposure and the dotted line is the spectrum taken after the sample is exposed to UV light. (a) Is  $H_2AA$  and  $Na_2AA$  supersaturated and no 6CN2. (b) Same concentration of  $H_2AA$  and  $Na_2AA$  with also  $1.0 \times 10^{-5}$  M 6CN2 added.**

Figure 3.3 is the emission spectrum of the buffered  $\text{H}_2\text{AA}/\text{HAA}^-$  solution with 6CN2 present resulting in no spectroscopic changes for excitation at 300nm if not exposed to light, representing the stability of spectroscopic properties of the 6CN2 fluorescing features. The 6CN2 in this solution has a  $\text{pH}$  that results in no spectroscopic features of the protonated excited state monomer and only the deprotonated anion is present. Another aliquot of the solution was exposed to the ultraviolet lamp and resulted in no significant spectroscopic changes for excitation at 300 nm.



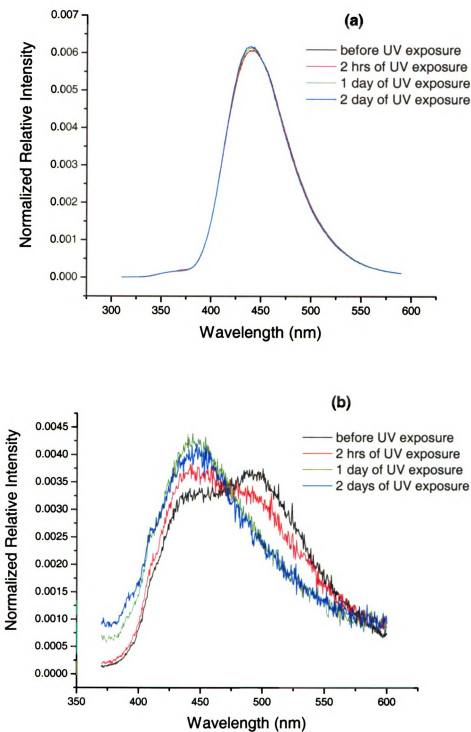
**Figure 3.3: Steady state spectra of 6CN2 in buffered  $\text{H}_2\text{AA}/\text{HAA}^-$  solutions for excitation at 300 nm with spectra taken in time intervals between 2 hrs to 12 hours. All spectra are identical. Solution not exposed to UV light.**

Essentially no spectroscopic changes were seen for excitation of the buffered  $\text{H}_2\text{AA}/\text{HAA}^-$  and 6CN2 solutions for excitation at 300 nm. However, spectroscopic changes in 6CN2 features did occur with constant light exposure for excitation at 360 nm. Samples were made and exposed to light under the same conditions stated above. Figure 3.4a represents the sample unexposed to ultraviolet light and resulted in no spectral changes with time, again confirming the photostability of 6CN2. Figure 3.4b has a sample exposed to light between the time span of 2 to 12 hours. There is the 440 nm emission peak, which is spectral overlap from the deprotonated monomer anion with an additional feature at 500 nm which decreased in intensity over constant light exposure. There is a possibility more excited state anions are being created over time as a result of the 440 nm peak increasing in intensity. The 500 nm peak maximum was found to shift to shorter wavelengths with increasing  $\text{pH}$  resulting in a combination of spectral overlap from the super photoacid anion monomer form and a complexation, which could be an aggregate as discussed in Chapter 2, or a complex between  $\text{H}_2\text{AA}$  and 6CN2.



**Figure 3.4: Steady state spectra of 6CN2 in buffered  $\text{H}_2\text{AA}/\text{HAA}^-$  solution with concentration ratio of  $\text{H}_2\text{AA}/\text{Na}_2\text{AA}$  10:1 for excitation at 360 nm with spectra taken in time intervals between 2 hrs to 12 hours after exposure. (a) Solution kept in the dark (b) Solution under UV exposure. Concentration of adipic acid to sodium adipate is 10:1.**

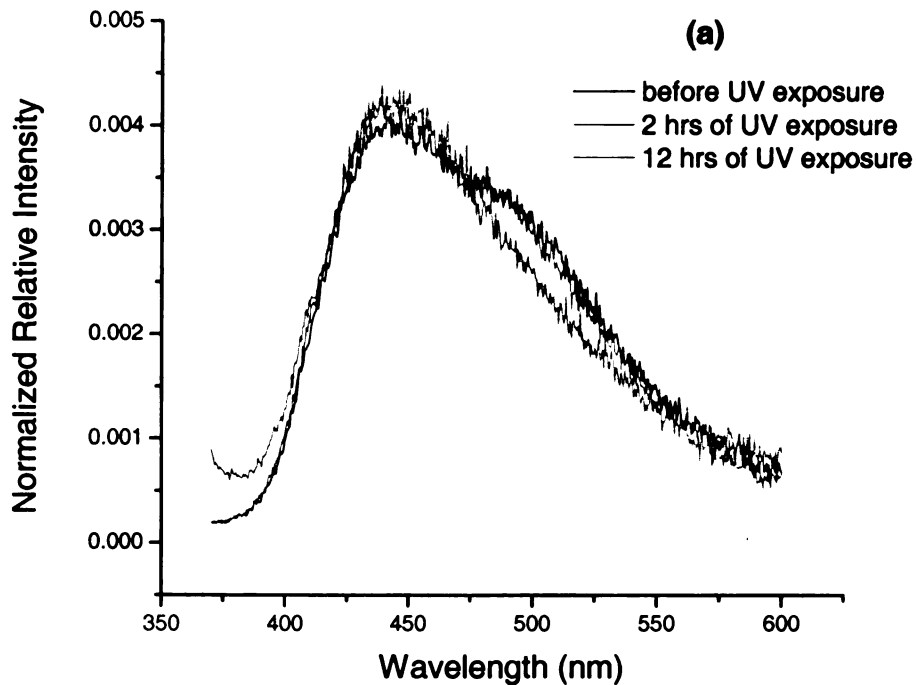
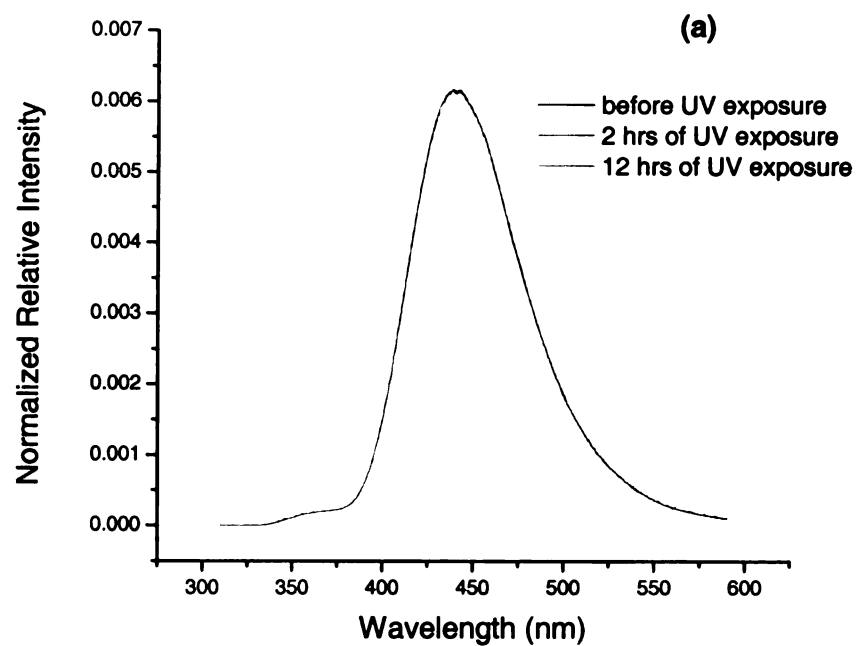
Various concentration ratios of  $\text{H}_2\text{AA}$  and  $\text{Na}_2\text{AA}$  for the buffered  $\text{H}_2\text{AA}/\text{HAA}^-$  solution with 6CN2 were investigated in steady state spectroscopy to determine if 6CN2 changed in its spectroscopic properties. Regardless of the concentration ratios of these two species, no spectral changes of 6CN2 for excitation at 300 nm were found. However, various concentration ratios of  $\text{Na}_2\text{AA}$  and  $\text{H}_2\text{AA}$  affected the spectral features of 6CN2 for excitation at 360 nm. The previous solutions analyzed were with a concentration ratio of  $\text{H}_2\text{AA}$  and  $\text{Na}_2\text{AA}$  of 10:1. Significant changes were found and investigated with a 30:1 concentration ratio of  $\text{H}_2\text{AA}$  to  $\text{Na}_2\text{AA}$  respectively. Aliquots of the solutions kept in the dark and analyzed under steady state conditions but are not shown since they are time invariant. Figure 3.5a is the sample excited at 300 nm and (b) is an emission spectrum of a sample excited at 360 nm for the 30:1  $\text{H}_2\text{AA}/\text{Na}_2\text{AA}$  ratio. By comparison of Figure 3.5b to Figure 3.4, the 500 nm emission peak is more prominent for  $\text{H}_2\text{AA}/\text{Na}_2\text{AA}$  ratios that were 30:1, as opposed to 10:1. Again, for excitation at 300nm, there are no spectral changes in 6CN2 fluorescence spectrum with varying concentration ratios of  $\text{H}_2\text{AA}/\text{Na}_2\text{AA}$ .



**Figure 3.5: Steady state spectra of 6CN2 with H<sub>2</sub>AA/Na<sub>2</sub>AA concentration ratio 30:1 and under UV exposure. The buffered H<sub>2</sub>AA/HAA<sup>-</sup> and 6CN2 solution (a) 300 nm excitation (b) 360 nm excitation.**

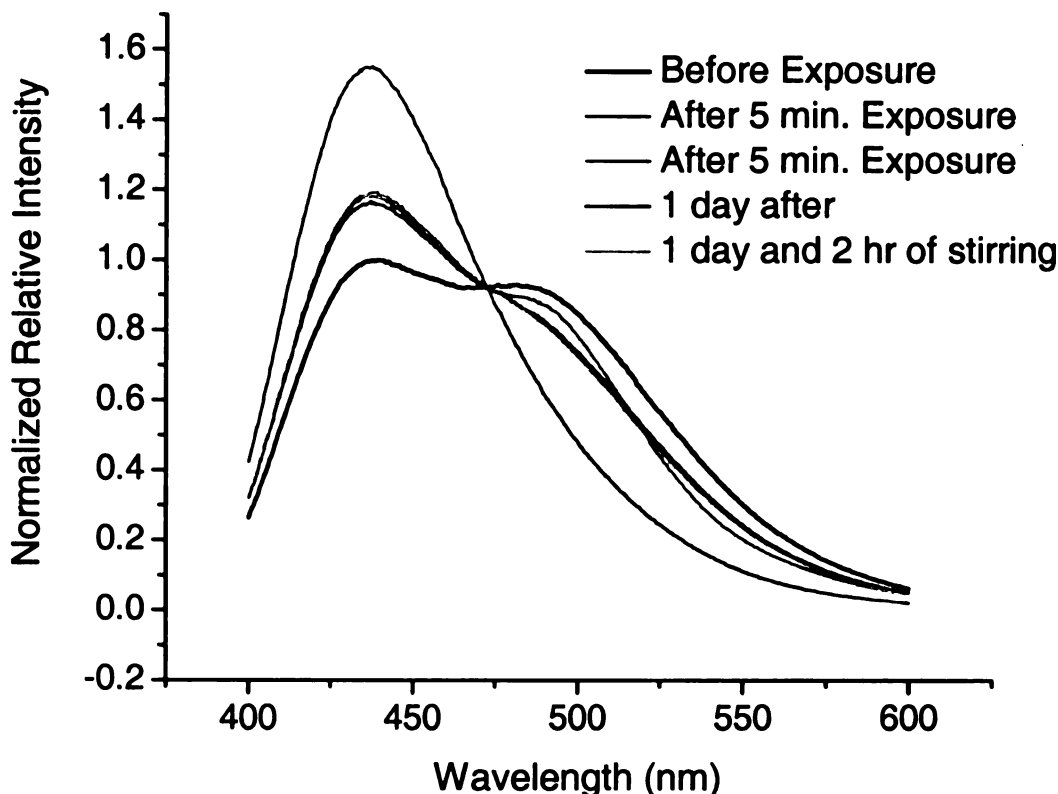


Figure 3.6 is an emission spectrum of a solution of only  $\text{H}_2\text{AA}$  and 6CN2 exposed to ultraviolet light and monitored with steady state spectroscopy for excitations at 300 nm and 360 nm. The solution was prepared as stated above to ensure the system was saturated with  $\text{HAA}^-$  molecules. Figure 3.6a represents that there is no spectral change for excitation at 300 nm. Figure 3.6b is for excitation at 360 nm. In comparison with the other concentration ratios, the spectral feature at 500 nm is less pronounced with no  $\text{Na}_2\text{AA}$  present. In Chapter 2 it was discussed that there is a possible aggregate formation at low  $\text{pH}$  for 6CN2, and it resulted in spectral features at 500 nm emission for excitation at 360 nm. It was discussed that at 500 nm emission there is possible complex formation and there is greater chance of a complex formation with the addition of  $\text{Na}_2\text{AA}$  to be included to make the buffered  $\text{H}_2\text{AA}/\text{HAA}^-$  solution. By showing the three different concentration ratios of  $\text{H}_2\text{AA}/\text{Na}_2\text{AA}$ , the optimal concentration of the buffered system to monitor any changes is with the 30:1 concentration. However, even though this ratio may be optimum to monitor spectral changes, the optimal concentration to have the 6CN2 initiate the crystallization event upon excitation still needs to be investigated. So far, no concentration ratios with 6CN2 present resulted in initiating crystallization of  $\text{H}_2\text{AA}$ .



**Figure 3.6: Steady state spectra 6CN2 and H<sub>2</sub>AA with no Na<sub>2</sub>AA added in aqueous solution exposed to UV light. The buffered H<sub>2</sub>AA/HAA<sup>-</sup> solution (a) for excitation at 300 nm (b) for excitation at 360 nm.**

Another experiment was performed to investigate after 10 minute constant exposure to 350 nm laser light beam path to see if the system was reversible with the proton donation from the super photoacid (Figure 3.7). The spectral feature at 500 nm diminishes after constant ultraviolet lamp exposure and the 440 nm emission peak increases in intensity. When the sample with all three components in the solution is constantly exposed at 355 nm, the solution fluoresces from green to blue in the path length of the light as well as tiny particles were moving around in solution. A 250 mL buffered  $\text{H}_2\text{AA}/\text{HAA}^-$  solution with 6CN2 present was irradiated for excitation 355 nm by the laser for 30 minutes. There was no precipitation that resulted in the bottom of the flask suggesting no definite determination that enough  $\text{H}_2\text{AA}$  was added to precipitate out of solution. After constant 355 nm exposure, the sample was removed and allowed to sit in the dark. After 12 hours, a steady state spectrum was collected for excitation 360 nm the 500 nm peak that had disappeared had returned and the 440 nm peak had diminished in intensity. This 500 nm spectral feature did not return to its original intensity prior to exposure. The solution was then stirred for 2 hours and another steady state spectrum was collected at 300 nm and yielded the same spectral features as the one 2 hours prior. The 500 nm feature never returns fully to its original bandshape prior to UV exposure, suggesting that the system is partially irreversible. When the 6CN2 in the buffered  $\text{H}_2\text{AA}/\text{HAA}^-$  solution is exposed to UV light, it causes proton donation to the adipate anion, which based on the spectroscopic data is not fully reversible even on day long time frames.



**Figure 3.7: Steady state spectra 6CN2 in buffered  $\text{H}_2\text{AA}/\text{HAA}^-$  solution for excitation at 350 nm. The solution was exposed to 355 nm UV light powered by a laser for 5 minutes and then allowed to sit in the dark after exposure.**

No visible precipitate was found, but that is not to say that very small crystallites or rather aggregates are not forming. The Blanchard lab is not equipped to detect such a species forming after excitation of 6CN2 in the buffered  $\text{H}_2\text{AA}/\text{HAA}^-$  solution. One possibility that no precipitate was found could be the concentrations of each species in solution were not correct to push the adipic acid to nucleate and form a precipitation event to occur. If the solution did not have enough  $\text{HAA}^-$  accepting protons, then the probability for the  $\text{H}_2\text{AA}$  molecules that did form to come in contact with one another and form a

nucleation site is extremely small. The other factor discussed in affecting crystal growth was particle size and if there are relatively few  $\text{H}_2\text{AA}$  formed, the particle size is probably small resulting in little chance for crystallization to occur. The spectroscopic changes of 6CN2 for excitation at 360nm show that there is a permanent change signifying the possibility that a proton was donated to the solution and possibly  $\text{H}_2\text{AA}$  was formed.

*Time correlated single photon counting (TCSPC).* Time domain studies were performed with 6CN2 in aqueous solutions with a concentration ratio of  $\text{H}_2\text{AA}$  and  $\text{Na}_2\text{AA}$  to be 30:1 and also one with  $\text{H}_2\text{AA}$  and 6CN2 in the solution. When these mixtures were prepared and placed in the path of the light for the TCSPC and it was excited at 300 nm the solution fluoresces a bright green.

Table 3.1 shows the lifetimes of buffered  $\text{H}_2\text{AA}/\text{HAA}^-$  solutions with  $10^{-5}$  M 6CN2 present. The longer lifetime values resemble those near a similar pH 6CN2 not in a buffered system, and reported in Chapter 2. Figure 3.8 shows the raw data collected of a buffered sample with the adipic acid to sodium adipate concentration ratio 30:1. The lifetimes fit a biexponential decay and the values are similar to the values reported in Chapter 2, suggesting the spectroscopic time domain features of 6CN2 is not altered much in the presence of  $\text{H}_2\text{AA}$ ,  $\text{HAA}^-$ , and  $\text{AA}^{2-}$  in the solution. The fluorescence lifetime is the same with  $\text{Na}_2\text{AA}$  present in the solution and with it not present in the solution.

**Table 3.1: Lifetime values of buffered H<sub>2</sub>AA/HAA<sup>-</sup> solutions with 1.0 x 10<sup>-5</sup> M 6CN2. Excitation at 300 nm.**

<b>Excitation 300nm</b>	<b>A<sub>1</sub></b>	<b>τ<sub>1</sub></b>	<b>A<sub>2</sub></b>	<b>τ<sub>2</sub></b>
<i>Emission 440nm</i>				
Buffered Solution	0.61	6049 ± 55	-0.39	192 ± 7.40
Solution, No Na <sub>2</sub> AA	0.62	5905 ± 39	-0.38	180 ± 4.80

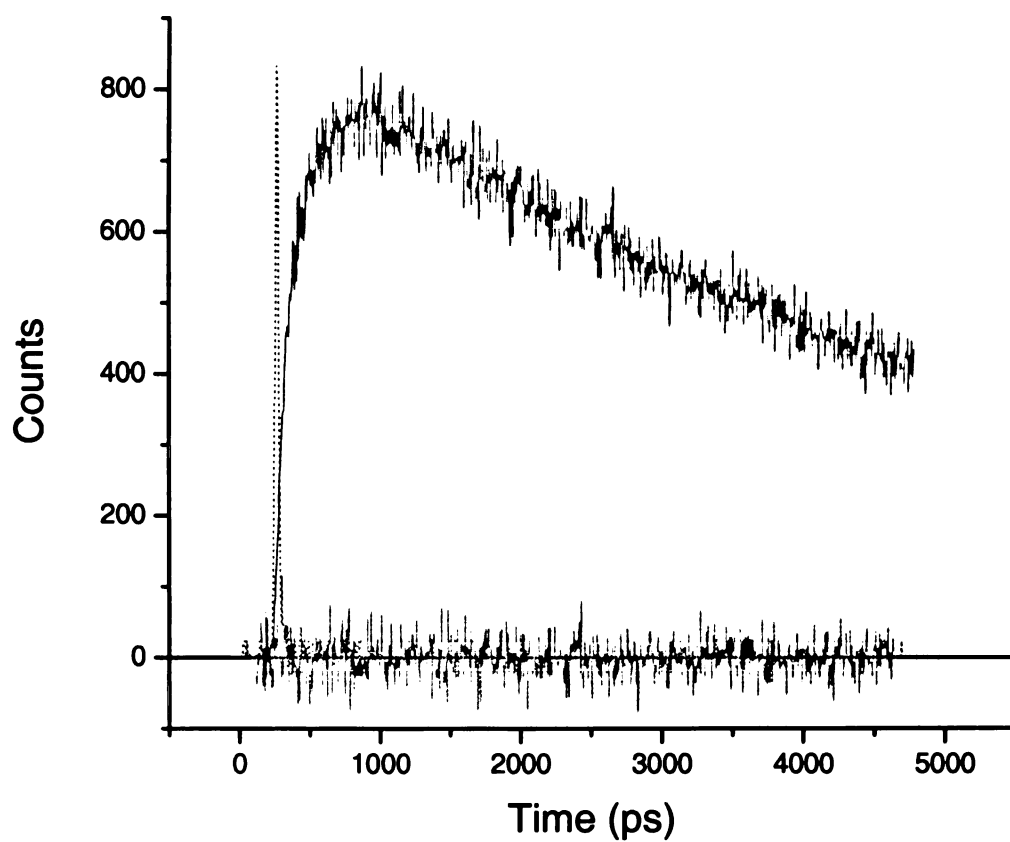


**Figure 3.8: TCSPC data for excitation at 300nm, emission at 440nm. Buffered H<sub>2</sub>AA/HAA<sup>-</sup> solution with concentration ratio of H<sub>2</sub>AA and Na<sub>2</sub>AA 30:1. The 6CN2 was in 1.0x10<sup>-5</sup>M concentration.**

Figure 3.9 has similar information as Figure 3.8, except there is no  $\text{Na}_2\text{AA}$  present in the aqueous solution. Initial inspection of the spectra, without looking at the exponential fit results appears no significant spectral changes happened for excitation at 300 nm and collection at 440 nm. Tables 3.1 reports the lifetime information, which shows upon comparison to values found in Chapter 2, resemble lifetime values for  $\text{pH}$  greater than 3. Table 3.2 is investigating if the anisotropy of 6CN2 changes when other species are present in the system. The reorientation information is extracted from fluorescence intensity decays polarized parallel and perpendicular to the vertical excitation polarization. Table 3.2 shows the anisotropy values for these systems, and they correspond to what happens for molecules in aqueous systems. In fact, when comparing to our values in Chapter 2 and noting the  $\text{pH}$ , our data in a buffered system at excitation 300nm is in excellent agreement with our previous results. It only shows that at this  $\text{pH}$  there is only a monomer form present of the solution. This is consistent with our steady state spectra, that the concentration of  $\text{H}_2\text{AA}$  and  $\text{Na}_2\text{AA}$  does not affect the spectroscopic features of 6CN2 for excitation at 300 nm.

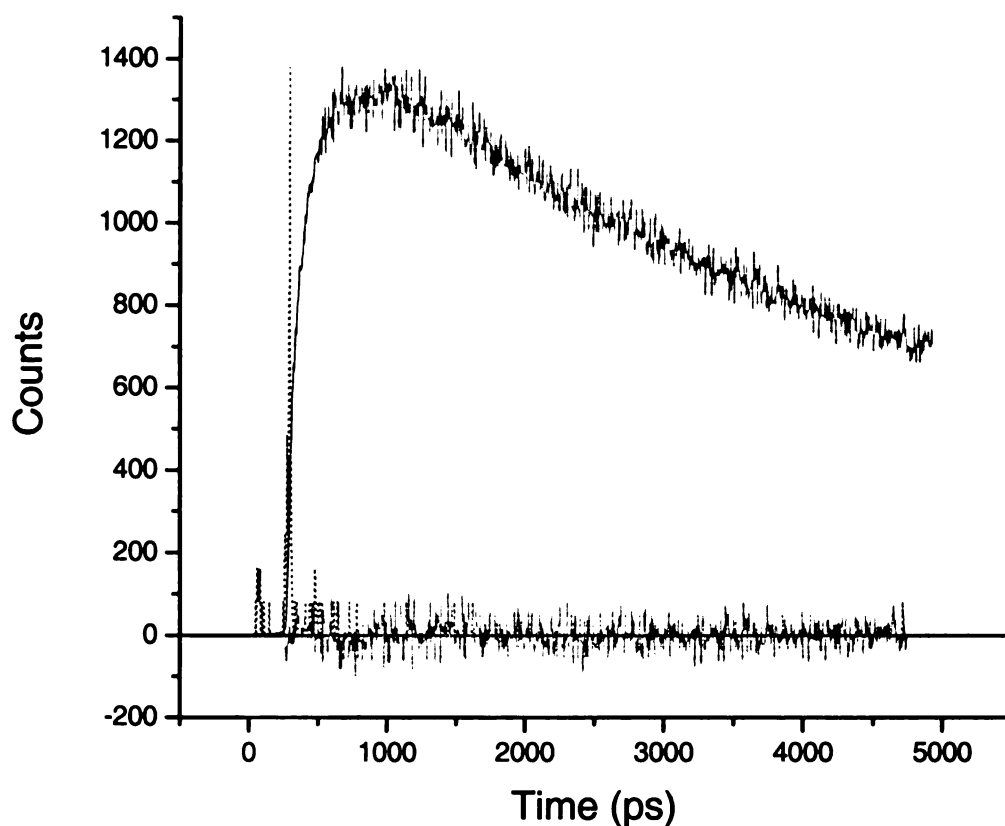


**Figure 3.9:** Lifetime of H<sub>2</sub>AA solution with no Na<sub>2</sub>AA and 10<sup>-5</sup> M 6CN2 for excitation at 300nm emission collection at 440 nm.

**Table 3.2:** Anisotropy values for buffered system with 6CN2 In solution. Excitation 300 nm, emission collection 440nm

Excite 300nm	R(0)	$\tau_{OR}$
<i>Emission 440nm</i>		
Buffered solution	$0.160 \pm 0.021$	$89 \pm 13$
Solution, no Na <sub>2</sub> AA	$0.1600 \pm 0.0098$	$72 \pm 5.40$

No buffered H<sub>2</sub>AA/HAA<sup>-</sup> solutions with 6CN2 were analyzed with TCSPC for excitation at 360nm because at this excitation, there fluorescence signal was weak and therefore could not be detected from the detection for the TCSPC system. The time domain spectra collected at this excitation for these buffered





solutions had a high signal to background ratio, making it difficult to analyze the decay function of the molecule.

### 3.4 Conclusion

The buffered  $\text{H}_2\text{AA}/\text{HAA}^-$  solution does not fluoresce unless 6CN2 is added. Over a period of 12 hours, 6CN2 in the buffered  $\text{H}_2\text{AA}/\text{HAA}^-$  solution appears to remain stable if it is not exposed to constant ultraviolet light for either excitation at 300 nm or 360 nm. However, upon constant ultraviolet exposure, the 6CN2 in the buffered  $\text{H}_2\text{AA}/\text{HAA}^-$  solution does not result in significant changes for excitation at 300 nm. In fact, it resembles the spectrum of 6CN2 in an aqueous solution that is above  $\text{pH}=3$ . However, the concentration ratio of  $\text{H}_2\text{AA}/\text{Na}_2\text{AA}$  present in the buffered solution does affect the spectroscopic properties of 6CN2 in solution after ultraviolet exposure for excitation at 360nm. In fact there is possibly a complexation between 6CN2 and the adipate anion. This complexation is probably with hydrogen bonding in nature. This complex is 500 nm emission and the complex probably breaks apart upon constant ultraviolet light exposure. It was also found that using a laser to expose the buffered  $\text{H}_2\text{AA}/\text{HAA}^-$  solution, the proton donation to the solution is partially irreversible suggesting a proton is leaving the super photoacid 6CN2 and possibly going to the  $\text{HAA}^-$  in the solution and forming  $\text{H}_2\text{AA}$ . Even though  $\text{H}_2\text{AA}$  is possibly formed, the particle size is probably not large enough to help create a nucleation site and initiate a crystallization event to happen.

It is not known how many protons are donated to the system per adipic acid molecule that is formed. This would require much more in depth detailed analysis. More studies with varying the concentration levels each species in the buffered solution would need to be investigated to help encourage the crystallization of adipic acid.

### 3.5 Literature Cited

1. Mullin, J. W. *Crystallization*; Butterworth-Heinemann: Oxford, England, **1993**.
2. Myerson, A.S.; Sorrel, L.S.; *AIChE J.* **1982**, *28*, 778
3. Sorrel, L.S.; Myerson, A.S.; *AIChE J.* **1982**, *28*, 772
4. Chang, Y.C.; Myerson, A.S.; *AIChE J.* **1985**, *31*, 980
5. Chang, Y.C.; Myerson, A.S.; *AIChE J.* **1986**, *32*, 1567
6. Chang, Y.C.; Myerson, A.S.; *AIChE J.* **1986**, *32*, 1747
7. Larson, M. A.; Garside, J.; *Chem. Eng. Sci.* **1986**, *41*, 1285
8. Larson, M. A.; Garside, J.; *J. Crystal Growth.* **1986**, *76*, 88
9. Kohan, M.I. *Nylon Plastics*, J. Wiley & Sons: New York **1973**
10. Luedeke, V., McKetta J. and Cunningham, W. (Ed). *Encyclopedia of Chemical Processing and Design*, **1977**, *2*, 128
11. *Kirk-Othmer*, 4<sup>th</sup> ed., *1*, 466
12. Sittig, M. *Dibasic acids and anhydrides*, Noyes Development Corp: NJ **1966**
13. Chakraborty, R.; Berglund, K. A.; *AIChE. Symp. Ser.* **1991**, *284*, 113
14. Rasimas, J.P.; Berglund, K. A.; Blanchard, G. J.; *J. Phys. Chem.* **1996**, *100*, 7220
15. Rasimas, J.P.; Berglund, K. A.; Blanchard, G. J.; *J. Phys. Chem.* **1996**, *100*, 17034
16. Tulock, J. J.; Blanchard, G. J.; *J. Phys. Chem. B* **1998**, *102*, 7148
17. Tulock, J. J.; Blanchard, G. J.; *J. Phys. Chem. A* **2000**, *104*, 8340
18. Kelepouris, L.; Blanchard, G. J.; *J. Phys. Chem. A* **2000**, *104*, 7261
19. Skoog, D.A.; Holler, F.J.; West, D. M.; *Analytical Chemistry: An Introduction* 7<sup>th</sup> Ed. Harcourt, Inc. Orlando, Florida **2000** 182
20. DeWitt, L.; Blanchard, G. J.; LeGoff, E.; Benz, M. E.; Liao, J. H.; Kanatzidis, M. G. *J. Am. Chem. Soc.*, **1993**, *115*, 12158.

## Chapter 4

### Conclusions and Future Work

#### 4.1 Conclusions

Inducing a crystallization event by optical means is a complicated task. There are many factors to consider including solute concentration, solubility, type of crystallization initiator, the initiation event, and how to monitor the crystallization process. In order to try to control crystallization through an optically induced event using a photoacid, the solubility of the solute chosen would have to be *pH* dependent. The initiator we have chosen was 6-cyano-2-naphthol, a “super” photoacid that has a strong electron withdrawing group on the distal ring of the naphthol. The buffered system chosen was a solution of 6CN2 with adipic acid and sodium adipate so that the system could be driven into supersaturation by photoexcitation of 6CN2.

The super photoacid's protonation and deprotonation kinetics are not simple and in order to use it successfully in a buffered system to induce a crystallization event, the molecule itself needs to be characterized. The protonation and deprotonation dynamics were studied for the 6-cyano-2-naphthol at various *pH*s and the time-resolved lifetime and anisotropy data were also obtained for 300 nm excitation and 360 nm excitation for different *pH* solutions. It was found in the time domain data that for 300 nm excitation, very acidic solutions kept the proton on 6CN2 within the first 500 ps of the molecule after excitation. Basic solutions on the other hand, showed a protonated form at very

early times with a decrease in the protonated band to a corresponding rise in the 440 nm band within the first 500 ps. For the 350 nm excitation data, with the TCSPC, it was found that acidic solutions had a peak corresponding to 500 nm steady state spectra and a peak at 440 nm emission, which is the deprotonated excited monomer anion. The 500 nm peak could be a complexation of 6CN2 as well as the protonated/deprotonated species of 6CN2 in aqueous solution. We have concluded that it is an aggregate of the protonated forms that exists in acidic conditions, however, the lifetime of this molecule is extremely short.

For 360 nm excitation, the fluorescence intensity of 6CN2 is not as high as exciting 6CN2 for 300 nm excitation. There is no evidence supporting the existence of an aggregate species in basic solutions. The 6CN2 for excitation at 360 nm barely fluoresced especially in acidic solutions, which makes it difficult to obtain useful TCSPC measurements. With the buffered  $\text{H}_2\text{AA}/\text{HAA}^-$  and 6CN2 solutions, no spectral change occurs for excitation at 300nm and constant UV exposure; since the  $\text{pH}$  of this solution is where the excited state monomer of the anion of 6-cyano-2-naphthol is present. Spectral changes were observed with the buffered solutions of  $\text{H}_2\text{AA}/\text{HAA}^-$  and 6CN2 and constant UV exposure. Concentration ratios were altered of the  $\text{H}_2\text{AA}$  and  $\text{Na}_2\text{AA}$  present in the system to ensure the solution had  $\text{HAA}^-$  present in the system. In the TCSPC measurements, only 300 nm excitation was studied and it was found that no major spectroscopic changes happened in the time domain in regards to the lifetime of 6CN2 in solution. The major spectroscopic changes observed of  $\text{H}_2\text{AA}$  and  $\text{Na}_2\text{AA}$  in solution were observed with steady state spectroscopy.

Theoretically the proton would come off of the super photoacid and attach to the  $\text{HAA}^-$  that is present in the buffered  $\text{H}_2\text{AA}/\text{HAA}^-$  forming  $\text{H}_2\text{AA}$ . If enough  $\text{H}_2\text{AA}$  were formed, then possibly a nucleation site would form and crystallization event would have been initiated. However, as of yet, a crystallization event has not been observed. Therefore more studies need to be done on the complexation events between adipic acid, sodium adipate, and the 6-cyano-2-naphthol that are present in the aqueous solution. .

## **4.2 Future Work**

More analysis needs to be done to understand the equilibrium between the dimer formation and the monomer of the 6-cyano-2-naphthol. The other equilibrium needed to be studied is from the excited state monomer back into a possibly ground state protonated form and an excited state deprotonated form. Once this information is found out then a very complete picture of the complicated equilibrium studies can be obtained and applied and the 6-cyano-2-naphthol can be used more effectively as a crystallization initiator in various systems.

Adipic acid in a buffered solution was originally a good choice because its crystallization events have been studied extensively by former Blanchard lab members.<sup>1-5</sup> It is quite possible that this weak acid is not a good choice; because of the likely-hood that it could form an ester complex, since it is a polyprotic carboxylic acid. In order to make this optical crystallization initiation event to work, it might be more beneficial to study different weak acids that are more sensitive to accepting protons in aqueous solution. It could also be that even

though the  $pK_a$  to  $pK_a^*$  jump is rather large for the photoacid, the  $pH$  regime we were working in was too basic and so it would be beneficial to find a different weak acid that works in a more acidic  $pH$  region and then go back to the adipic acid system, once simpler systems are understood.

The 6-cyano-2-naphthol can also be used for biological systems that are  $pH$  dependent. It can be used as a probe with systems since the protonated and deprotonated dynamics are understood with this super photoacid. As long as the  $pH$  is kept basic enough, then there will be no complexation of an aggregate species present to be worrying about.



### **4.3 Literature Cited**

1. Rasimas, J.P.; Berglund, K. A.; Blanchard, G. J.; *J. Phys. Chem.* **1996**, *100*, 7220
2. Rasimas, J.P.; Berglund, K. A.; Blanchard, G. J.; *J. Phys. Chem.* **1996**, *100*, 17034
3. Tulock, J. J.; Blanchard, G. J.; *J. Phys. Chem. B* **1998**, *102*, 7148
4. Tulock, J. J.; Blanchard, G. J.; *J. Phys. Chem. A* **2000**, *104*, 8340
5. Kelepouris, L.; Blanchard, G. J.; *J. Phys. Chem. A* **2000**, *104*, 7261

MICHIGAN STATE UNIVERSITY LIBRARIES



3 1293 02732 5012